Journal Pre-proofs

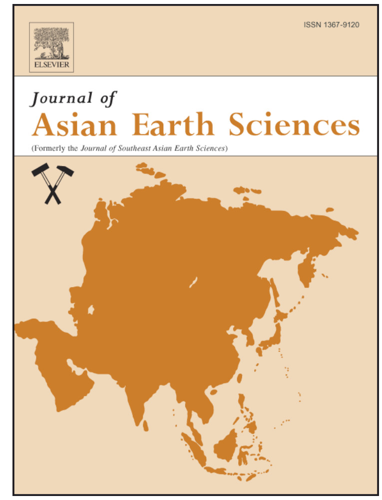

A Multi-Proxy Provenance Study of Eocene to Oligocene Sandstones in the Salin Sub-basin, Myanmar

Joseph D. McNeil, Amy Gough, Robert Hall, Nils Keno Lünsdorf, Max Webb, Sarah Feil

PII: S1367-9120(21)00163-2
DOI: https://doi.org/10.1016/j.jseaes.2021.104825
Reference: JAES 104825

To appear in: *Journal of Asian Earth Sciences*

Received Date: 6 November 2020
Revised Date: 27 April 2021
Accepted Date: 10 May 2021

Please cite this article as: McNeil, J.D., Gough, A., Hall, R., Keno Lünsdorf, N., Webb, M., Feil, S., A Multi-Proxy Provenance Study of Eocene to Oligocene Sandstones in the Salin Sub-basin, Myanmar, *Journal of Asian Earth Sciences* (2021), doi: https://doi.org/10.1016/j.jseaes.2021.104825

A Multi-Proxy Provenance Study of Eocene to Oligocene Sandstones in the Salin Sub-basin, Myanmar

Joseph D. McNeil*[a,b]; Amy Gough[a]; Robert Hall[a]; Nils Keno Lünsdorf[c]; Max Webb[a]; Sarah Feil[a]

a. SE Asia Research Group, Department of Earth Sciences, Royal Holloway University of London, Egham, Surrey, TW20 0EX, United Kingdom
b. School of Physical Sciences, The Open University, Milton Keynes, Buckinghamshire, MK7 6AA, United Kingdom
c. Department of Sedimentology and Environmental Geology, Georg-August-University Göttingen, Germany

*Corresponding Author: joe.mcneil@open.ac.uk

Abstract

The Salin Sub-basin, Myanmar, contains up to 15,000 metres of Cenozoic sediments, but their provenance remains ambiguous. Here, a multi-proxy provenance study that employed Raman Spectroscopy-assisted heavy mineral analysis, light mineral petrography, and U-Pb detrital zircon geochronology, is used to identify source areas and sediment pathways of nine samples from three formations of Eocene to Oligocene age. The heavy mineral assemblages are diverse and highly immature and indicate that sediments were principally provided from a range of igneous and metamorphic lithologies, with some recycling of older sediments. The metamorphic basement rocks in northern Myanmar are identified as a source in all three formations, suggesting that the headwaters of the sedimentary pathway were situated in this area. Detrital zircons overwhelmingly yield Cretaceous and Palaeogene ages. A population of Late Cretaceous and Palaeocene zircons could indicate input from the Mogok Metamorphic Belt, or a currently buried section of the Wuntho-Popa Arc; the diminishing of this signal by the end of the Rupelian suggests reduction in transport from the former, or burial of the latter. Late Cretaceous grains exhibit rounded and euhedral morphologies, suggesting input from recycled Wuntho-Popa Arc material via the sediments of the Chin Hills, and direct input from the Wuntho-Popa Arc, respectively. A persistent Palaeoproterozoic and Triassic signal in the Shwezetaw and Padaung Formations suggests provenance in the Pane Chuang Formation of the Indo-Myanmar Ranges, showing that by the early-mid Oligocene, the ranges were topographically prominent enough to be an important source of sediment for the Central Myanmar Basin.

Keywords: Sedimentary Provenance, Myanmar, U-Pb Zircon Geochronology, Raman Spectroscopy, Palaeogene

1. Introduction

The Salin Sub-basin is the deepest sub-basin of the Central Myanmar Basin, and has amassed approximately 15,000 m of sediment since the Late Cretaceous (Pivnik et al., 1998). Despite the great thickness of this accumulation, there are remarkably few provenance studies relevant to the sub-basin's Cenozoic stratigraphy. Previous provenance studies in the region (e.g. Garzanti et al., 2016) have primarily focused on the sedimentary routing systems of the modern Irrawaddy River, with only a few studies concerned specifically with the provenance of the Cenozoic strata (Licht et al., 2014c; Zhang et al., 2019). In the wider area, provenance studies have typically focussed on the strata of the Indo-Myanmar Ranges (Allen et al., 2008; Najman et al., 2020; Sevastjanova et al., 2016) and the Chindwin Basin (Kyaw Linn Oo et al., 2015; Licht et al., 2019; Westerweel et al., 2020) due to the good outcrop exposure and ease of access; others have concentrated on the Eocene strata in the centre of the basin as they contain numerous early anthropoids and are of global palaeontological importance (e.g. Jaeger et al., 1999; Takai et al., 2001; Beard et al., 2009; Chaimanee et al., 2012). Other studies have utilised zircon U-Pb geochronology to constrain the age of these fossil-bearing formations (Tsubamoto et al., 2002) or understand palaeo-drainage systems (Robinson et al., 2014; Zhang et al., 2019), but only one has focused specifically on the provenance of the Oligocene-Miocene Pegu Series in the Salin Sub-basin (Naing Htun Lin et al., 2019). Deposition of the Pegu Series occurred during a critical period in Myanmar's geological evolution. At this time, the Indo-Myanmar Ranges were starting to become topographically significant, and in the far north, the Eastern Himalayan Syntaxis continued its development as India moved northwards into Asia. Because the age of the Pegu Series spans the majority of this crucial time period, its detrital components could constrain the uplift and denudation of the IMR, the distant Eastern Himalayan Syntaxis, or show evidence of input from the east in the Sino-Myanmar Ranges.

Multi-proxy sedimentary provenance studies employing heavy mineral analysis and detrital zircon geochronology in tandem have markedly improved our understanding of erosional histories, palaeo-drainage pathways, and palaeogeography around the globe (Strnad and Mihaljevič, 2005; Mange et al., 2010; Sevastjanova et al., 2016). However, detrital heavy mineral analyses of the Cenozoic sediments in the Central Myanmar Basin are rare. Considering the lithological diversity of the terranes surrounding the Central Myanmar Basin, and the proven utility of heavy mineral studies in Southeast Asia (e.g. Galin et al., 2017; Hennig et al., 2018), a comprehensive study of the detrital heavy minerals in the Cenozoic strata could provide important information concerning the geologic development of the Central Myanmar Basin. This study presents the first combined heavy mineral and geochronological analyses of the Pondaung, Shwezetaw and Padaung Formations of the Salin Sub-basin, in order to: 1) identify source regions based on heavy mineral studies and detrital zircon U-Pb geochronology; 2) understand the sedimentary routing pathways of the formations; and 3) better constrain the maximum depositional ages of the major formations, which are currently predominantly based on limited biostratigraphy.

2. Geologic Setting

The geology of Myanmar is principally the result of two major geological processes: firstly, the Late Palaeozoic to Mesozoic accretion of continental arc and ophiolite terranes to form Southeast Asia (Mitchell, 1981; Hutchison, 1989; Metcalfe, 1996; Hall, 2002), and secondly, the convergence of the Indian plate, Myanmar microplate, and Eurasian plate in the ongoing Himalayan Orogeny (Mitchell, 1981, 1989; Satyabala, 2003). In Myanmar, these events have produced a tectonically complex region containing diverse lithologies that are primarily Mesozoic and Cenozoic in age. Myanmar can be physiogeographically subdivided into three north-south trending terranes: 1) the Indo-Myanmar Ranges (IMR), a fold-thrust belt interpreted as an accretionary complex comprising Mesozoic to Cenozoic Bengal Fan sediments, medium-grade metamorphics and ophiolitic suites that formed as a result of the oblique subduction of the Indian plate beneath Myanmar during the Cenozoic (Brunnschweiler, 1966; Curray, 1989; Maurin and Rangin, 2009; Westerweel et al., 2019); 2) the Sino-Myanmar Ranges, a section of the Sibumasu block that includes the Mogok Metamorphic Belt (MMB), composed primarily of Palaeozoic sediments, metasediments, and granitic plutons (e.g. Bender, 1983; Searle et al., 2017, 2007, 2020); and 3) the Central Myanmar Basin (CMB), an elongate depression containing more than 15,000 m of Cenozoic sediments (Fig. 1).

2.1. The Indo-Myanmar Ranges

The IMR are divided into an outer wedge, comprising a fold-thrust belt made of Neogene Himalayan-derived Bengal Fan sediments (Steckler et al., 2008; Najman et al., 2012; Betka et al., 2018) and an inner wedge, comprising a basement of Triassic Pane Chaung Formation sediments and Kanpetlet Schists that are overlain by a series of Cretaceous-Eocene turbidites (Maurin and Rangin, 2009; Bannert et al., 2011; Mitchell, 2017), which are in turn unconformably overlain by Eocene-Oligocene molasse deposits (Bannert et al., 2011; Ghose et al., 2014; Morley et al., 2020). The CMB-adjacent inner wedge of the IMR is thought to have partially uplifted in the late

Eocene as evidenced by deposition in a quasi-closed estuarine environment constrained by this partial uplift (Licht et al., 2019) and coeval deposition of Eocene-Oligocene molasse deposits in the IMR. This was followed by major exhumation at the Eocene-Oligocene boundary (Najman et al., 2020). This switch is mirrored in the sedimentology and depositional environments (Gough et al., 2020; Westerweel et al., 2020) and corroborated by low temperature thermochronology (Najman et al., 2020). Following this, there have been suggestions of uplift occurring as late as the Oligo-Miocene boundary (Najman et al., 2019).

2.2. The Sino-Myanmar Ranges

The Sino-Myanmar Ranges are the geographic region of eastern Myanmar that includes the Shan Plateau (part of the Sibumasu Block) and the Mogok Metamorphic Belt (MMB). The MMB is a 1450 km-long sliver of medium to high grade metamorphic rocks that are intruded by the Jurassic to Eocene plutons (Chhibber, 1934; Khin Zaw, 1990; Barley et al., 2003; Searle et al., 2007, 2017). Composed primarily of gneisses, schists, and marbles (Searle et al., 2007), the belt extends almost the entire length of Myanmar along the eastern margin of the Sibumasu Block. Metamorphism and subsequent exhumation of the MMB east of the CMB occurred in the Eocene-Oligocene (Barley et al., 2003; Mitchell et al., 2012; Searle et al., 2007, 2017).

2.3. The Central Myanmar Basin

The elongate basin that dominates the geographic centre of Myanmar has previously been referred to as the Central Burmese Belt (Chhibber, 1934) or the Central Burma Depression (Racey and Ridd, 2015), but is now commonly called the Central Myanmar Basin (Pivnik et al., 1998; Bertrand and Rangin, 2003; Hall and Morley, 2004; Hennig et al., 2018; Morley and Searle, 2017; Gough et al., 2020). The CMB (Fig. 2) is separated from the Sino-Myanmar Ranges in the east by the dextral strike-slip Sagaing Fault, and from the IMR in the west by the Kabaw Fault (e.g. Win Swe, 1981; Morley et al., 2020). The CMB is divided into several sub-basins, which are arranged into two broadly parallel north-south trending troughs (Bender, 1983). These troughs are separated by the Wuntho-Popa Arc (WPA), a discontinuous magmatic arc considered to be the eastern continuation of the Gangdese Arc (Ma et al., 2014; Wang et al., 2014) that is mainly buried by Neogene sediments (Pivnik et al., 1998; Zhang et al., 2017). The WPA consists of batholiths, andesitic intrusions and numerous isolated I-type plutons (Khin Zaw, 1990), with main magmatic phases between 90–108 Ma and 36–42 Ma (Li et al., 2019; Lin et al., 2019; Licht et al., 2020). A fore-arc/back-arc basin couplet, the CMB troughs formed as a series of pull-apart basins through wrench tectonics in the Eocene and Oligocene as the Myanmar microplate migrated northwards relative to Asia (Tankard et al., 1994; Licht et al., 2019; Westerweel et al., 2020). However, the true origin of the larger basin in which they reside remains enigmatic (Mitchell, 1993; Pivnik et al., 1998; Bertrand and Rangin, 2003; Racey and Ridd, 2015). Situated in the forearc trough to the east of the IMR and the west of the WPA, the Salin Sub-basin is divided from the Chindwin Sub-basin to the north by the topographic high of the Pondaung Ranges (Pivnik et al., 1998; Licht et al., 2019).

2.4. Myanmar's Ophiolite Belts

There are two primary ophiolite belts in Myanmar. The Western Ophiolite Belt is a series of dismembered ophiolites that crop out along the eastern margin of the IMR and in the Naga Hills, and was emplaced during the Palaeogene (Searle et al., 2017). The Eastern Ophiolite Belt was previously subdivided into two belts: a central belt in the Jade Mines Belt, including the mafic and ultramafic lithologies in the Indawgyi area to the southeast, and an eastern belt, encompassing the ophiolitic materials in the Tagaung-Myitkyina Belt. This ophiolite belt was emplaced prior to the middle Cretaceous (Brunnschweiler, 1966; Mitchell, 1993; Mitchell et al., 2015). West of the Salin Sub-basin, the ophiolites of the Western Ophiolite Belt include harzburgites and lherzolites (Soibam et al., 2015). The ophiolitic lithologies in the Naga Hills region in the northern IMR contain abundant podiform magnesiochromite in the ultramafic host rocks (Maibam et al., 2017). Relic Cr-spinel is common relic mineral in the Jade Mines region of the Eastern Ophiolite Belt, occurring in serpentinised dunites and peridotites, and within chlorite schists in near the Tawmaw region (Hla Htay et al., 2017). Maw-sit-sit (a kosmochlor-rich rock), amphibolites, actinolite schists and chlorite schists in this region contain up to 4 vol% Cr-spinel (Thet Tin Nyunt et al., 2017). Other rocks in the Jade Belt Region include extensive, complex crystalline glaucophane and garnet-mica schists (Thet Tin Nyunt et al., 2017).

3. Stratigraphy and Sedimentary Provenance

3.1. The Pondaung Formation

The Eocene Pondaung Formation is a ca. 2000 m thick (Fig. 3) sequence of mudstones, sandstones and conglomerates, and has been informally subdivided into two members: 'lower' and 'upper' (Aye Ko Aung, 2004).

The lower member is 1500 m thick and is characterised by grey-brown coarse-to-pebbly crossbedded litharenites (Saw Lwin, 1999) that contain marine molluscs at the base of the member (Bender, 1983). Polymictic, clast-supported conglomerate beds are subordinate and are 20 m thick on average, with clast lithologies including volcanic and plutonic rocks, serpentinites, medium-to-high grade metamorphics, biogenic carbonate and chert, and polycyclic sediments (Maung Maung et al., 2005). The litharenites are interbedded with variegated mudstones and palaeosols (Licht et al., 2014b). The palaeosols are vertisols with pseudo-gley features characteristic of two sub-environments: 1) a seasonal wetland landscape with actively aggrading avulsion belts, and 2) distal open-forested environments (Licht et al., 2014b). Fossil leaves and angiosperm wood are present near the top of this member (Aye Ko Aung, 2004; Licht et al., 2014a).

The upper member forms the top 500 m of the formation and is dominated by fine-to-medium grained beige-brown sandstones, with interbedded variegated mudstones similar to the lower member (Aye Ko Aung, 2004). This member is most notable for its considerable range (more than 20 genera) of terrestrial mammals, including a substantial number of early adapiform primates (e.g. Aung Naing Soe et al., 2002; Khin Zaw et al., 2014). The upper member was deposited in a fluvio-deltaic environment (Maung Maung et al., 2005). The mean palaeocurrent direction indicates that the average flow was towards 243° (Licht et al., 2013).

The mammalian fauna (Pilgrim, 1916; Ciochon and Holroyd, 1994), nanoplankton biostratigraphy (Hla Mon, 1999), and foraminiferal biostratigraphy (Bender, 1983) indicate a Bartonian age for the formation which must extend into the Priabonian based on zircon fission-track dating of a tuffaceous bed as 37.2 ± 1.3 Ma (1σ), 300 m below the upper gradational boundary with the overlying Yaw Formation (Tsubamoto et al., 2002). Slightly older LA-ICP-MS, U–Pb zircon ages of 40.31 ± 0.65 Ma and

40.22 ± 0.86 Ma were also reported from a tuffaceous bed in the Pondaung Formation (Khin Zaw et al., 2014).

3.2. The Yaw Formation

The ca. 500 m thick Yaw Formation primarily comprises horizontally-laminated mudstones and calcareous sands that locally contain silt-dominated, micritic packstone layers (Licht et al., 2014b, 2020). The formation records the first evidence for differentiation of the depositional environments of the Salin and Chindwin sub-basins and could record the onset of sub-basin partitioning (Licht et al., 2019). The Yaw Formation is interpreted as having been deposited in a partially isolated estuarine environment (Licht et al., 2019), but was not investigated in this study owing to a lack of suitable samples for provenance.

3.3. The Pegu Series

The Oligocene-Miocene Pegu Series is a 6500 m thick succession of interbedded sandstones, limestones, and shallow marine shales (Stuart, 1912). It consists of six formations, the lowermost of which are the Shwezetaw and Padaung Formations which were investigated in this study.

3.3.1. *The Shwezetaw Formation*

The Shwezetaw Formation (Fig. 4a) is approximately 1000 m thick (Fig. 3, Bender, 1983; Pivnik et al., 1998) with 914 m proven in core (Racey and Ridd, 2015), and has a gradational lower boundary with the Eocene Yaw Formation. The formation is dominated by fine-grained, well-sorted sandstones, and can be divided into two members: a ~750 m thick 'lower alteration member' (LAM), and a ~250 m thick 'upper sandstone member' (USM, Than Htut, 2017).

The LAM consists of grey-brown micaceous and carbonaceous shales intercalated with fine-grained sandstone beds (Bender, 1983). The shale beds are soft to moderately hard. The shales and sandstones contain marine bivalve and gastropod fragments, and exhibit current ripples (Than Htut, 2017). Up section, the sand content of the LAM increases (Than Nyunt and Chit Saing, 1978; Naing Htun Lin et al., 2019), with individual beds reaching up to 30 cm in thickness at the top of the member. Sandstones exhibit both horizontal and vertical burrows, as well as trough cross bedding and hummocky cross-stratification (Bender, 1983).

The USM consists of dark yellow-brown, thickly-bedded (5-30 cm), fine to medium-grained sandstones, occasionally interrupted by thin blue shales and rare quartz-pebble conglomerates. The sandstones show a fining-upwards sequence and exhibit parallel bedding, cross laminae, and both uni- and bi-directional ripples (Mitchell, 2017). Evaporite beds and fossil wood are present at the base of the member (Than Htut, 2017), and rare coal beds can also be seen (Vredenburg, 1921). The upper limit of this member is a gradational boundary at the base of the Padaung Formation.

The LAM consists of fluvial sediments in the north of the basin that are intercalated with well-vegetated overbank deposits elsewhere (Gough et al., 2020). The USM represents a transition to a mixed tidal-fluviatile regime with evidence for a deltaic system that grades into a moderate to high energy shallow marine environment (Racey and Ridd, 2015) in the southwest (Gough et al., 2020). The conglomeratic areas are suggested to represent delta-lobe progradation, and parts of the USM may represent beach-front facies (Day Wa Aung, 2012). Overall, the Shwezetaw Formation represents a transition from a regime dominated by fluvial deposits to one where marine and deltaic systems play a more significant role.

3.3.2. *The Padaung Formation*

The Padaung Formation (Fig. 4b) conformably overlies the Shwezetaw Formation and is overlain conformably by the Okhmintaung Formation. It has received considerably less attention in the literature than the Shwezetaw and Pondaung Formations. 1188 m of sediment has been proven in core (Fig. 3, Racey and Ridd, 2015).

The Padaung Formation contains two main alternating facies: thickly-bedded medium-grained micaceous sandstones, and dark silty shales (Clegg, 1938). The sandstones contain abundant flaser beds, and both uni- and bi-directional cross stratification, sinuous-crested ripples, and mudstone rip-up clasts (Wandrey, 2006). This formation changes laterally, and as a result, the reservoir quality is variable. The proportion of clastic material in the Padaung Formation increases towards the north of the Salin Sub-basin, but the sandstones in the southern areas are more thickly bedded and possess better reservoir qualities (Racey and Ridd, 2015). Bioturbation is visible on the bedding planes in the form of *Skolithos* (Gough et al., 2020). Near the base of the formation, mudstones are common and contain a significant proportion of calcareous material, including mollusc fragments, foraminifera, ostracods, and occasional corals (Eames, 1950; Maung, 1970; Racey and Ridd, 2015).

The Padaung Formation records the continuation of the marine regression that started in the Salin Sub-basin during the deposition of the Shwezetaw Formation (Gough et al., 2020). The lower section of the Padaung Formation has some fluvial input, particularly in the far north of the basin. A fluvial-tidal deltaic system in the north passes southwards into a shallow marine environment in the medial and southern sections of the basin (Gough et al., 2020). Within the upper parts of the formation the marine transgression is recorded by shallow marine sediments, and mixed carbonate clastics and fossiliferous carbonates which dominate the stratigraphy (Gough et al., 2020).

3.4. Provenance of the Formations

The Eocene sediment in the CMB is proposed to be derived from local sources to the east and north-east, based on: 1) predominantly west-southwest directed palaeocurrents in both the Chindwin and Salin Sub-basins (Licht et al., 2013, 2019), 2) rapid fluctuation between marine and terrestrial fluviodeltaic depositional environments (Licht et al., 2013; Kyaw Linn Oo et al., 2015), 3) heterogeneous Sr-Nd data (Licht et al., 2013, 2014c,), and 4) petrographic and geochronologic data suggesting input from a contemporaneous volcanic arc (Kyaw Linn Oo et al., 2015; Licht et al., 2019; Naing Htun Lin et al., 2019). These lines of evidence suggest derivation from the WPA and the MMB in the Eocene (Zhang et al., 2019).

However, Hf signatures of zircons from the Dianxi batholith in south China and the intrusions in the MMB along the Shan Scarp yield mainly negative values (Searle et al., 2017; Gardiner et al., 2018; Lin et al., 2019), while Eocene sediments in the CMB have predominantly positive Hf values (Wang et al., 2014; Zhang et al., 2019; Arboit et al., 2021). Miocene and younger CMB rocks display negative Hf values, suggesting a major switch in provenance occurred in the Oligocene (Zhang et al., 2019). Both Zhang et al. (2019) and Licht et al. (2019) imply that this switch occurred at some point during the Late Eocene or Early Oligocene, a time period covered in the Salin Sub-basin by the Pondaung, Shwezetaw and Padaung Formations.

Zhang et al. (2019) found that the Padaung Formation in the Salin Sub-basin records evidence for input from the MMB in the form of detrital rutile and mica ages, Hf signatures, bulk rock Sr-Nd and petrographic data. They prefer derivation from the northern sections of the MMB over the southern region, owing primarily to its larger size, slightly older U-Pb crystallisation ages, and the total lack of detrital carbonates in the CMB rocks, which are ubiquitous along the eastern edge of the MMB.

Clearly, the work of Zhang et al. (2019) and Licht et al. (2019) show that provenance data for the Shwezetaw Formation from the Salin Sub-basin is crucial for our understanding of Palaeogene sedimentary pathways in Myanmar. The Chindwin sub-basin contains no Lower Oligocene strata and records an unconformity at this time, and in the Salin Sub-basin, the Pondaung and Padaung Formations appear to mark a period of reorganisation of the sedimentary pathways. This study, therefore, provides a unique opportunity to further constrain the timing of this provenance switch.

4. Materials and Methods

Nine samples were used in this study. We analysed two samples from the upper Pondaung Formation, three samples from the Shwezetaw Formation representing the lower, middle and upper sections of the formation, one sample from the boundary between the Shwezetaw and the Padaung Formation, and three samples from the Padaung Formation representing the lower, middle, and upper sections of the formation (Table 1). Samples from the Yaw Formation were prepared but were not suitable for provenance analysis owing to their overwhelming sub-63 μm grain sizes.

The samples were collected from the outcrops that occupy the western margin of the Salin Sub-basin during the 2017 and 2018 field seasons. These outcrops possess excellent lateral outcrop continuity and good exposures of the target formations and are therefore desirable for sampling in a stratigraphic provenance study. Therefore, we are confident that our samples are stratigraphically well-located. All samples with the exception of MAG_18_10 were studied using light mineral petrography and heavy mineral analysis using a combination of Raman Spectroscopy and optical point counting. LA-ICP-MS U-Pb dating of detrital zircons was undertaken for all samples including MAG_18_10.

4.1. Sample Preparation

After thin-sections were prepared, approximately 1 kg of each sample was disaggregated using a tungsten-carbide mill with a plate separation of 0.10 mm. Half of the resultant coarse sand was sieved to retain the 250 μm and 63 μm fraction and washed multiple times to remove loose silt or mud grain coatings. The samples were then left to soak in 10% acetic acid to remove carbonate coatings and were washed for a final time before being dried. Magnetic components were removed using a hand-magnet. Heavy and light minerals were separated using LST with a density of 2.89 g cm^{-3}. One half of the resultant heavy mineral aliquot was retained for heavy mineral analysis. The second half was subject to further magnetic separation using a Frantz magnetic separator and a final density separation using DIM (di-iodomethane) at 3.31

g cm^{-3} to produce a final aliquot that consisted of zircon grains. Zircons were picked at random and placed on slides for analysis.

4.2. Light Mineral Analysis

Point-counting of light mineral grains was conducted at Royal Holloway, University of London (RHUL) according to the Gazzi-Dickinson method (Dickinson, 1985). Plagioclase was stained using barium chloride and amaranth solution and K-feldspar was stained using sodium cobaltinitrite. A minimum of 300 framework grains were randomly selected and counted using a Nikon Eclipse LV100 and a manual stepping stage.

4.3. U-Pb Zircon dating

CL images of the zircon separates were collected at the Scanning Electron Microscope (SEM) Facility at RHUL using a Hitachi S3000 SEM. U-Pb zircon geochronology of all samples except MAG_18_10 was conducted at University College London (UCL), using an Agilent 7700cs quadrupole-based ICPMS, attached to a New Wave 213 aperture-imaged frequency-quintupled laser ablation system (213 nm). U-Pb zircon geochronology of MAG_18_10 was conducted at RHUL using a custom designed deep-UV RESOlution M-50 193 nm Excimer laser ablation system coupled to an Agilent 7500ce/cs quadropole ICP-MS. Grains were ablated with a 40 µm laser spot at UCL and a 25 µm laser spot at RHUL. Plesoviče zircons (337.13 ± 0.37 Ma; Sláma et al., 2008) and NIST SRM 612 silicate glass (e.g. Pearce et al., 1997) standards were used to correct error induced by mass fractionation and instrumental bias. Glitter software (Griffin et al., 2008) was used to process the raw zircon U-Pb age data. Whenever possible, at least 100 grains were analysed from each sample; however, some samples yielded too few zircons and were combined where appropriate for the purposes of discussion of age data.

4.4. Raman Spectroscopy

Raman Spectroscopy was conducted at the Department of Sedimentology and Environmental Geology, University of Göttingen. A Zeiss Axio Imager 2 microscope was used to create two mosaics of the heavy mineral stubs, one in transmitted light, and one in reflected light. A Horiba XPloRA Plus spectrometer with a motorised x-y-z stage was used in conjunction with a 532 nm diode laser set to a maximum output power of 25 mW. Measurements were conducted with a confocal hole diameter and slit set to 100 µm with an 1800 l mm^{-1} grating and 100x 0.8 NA objective. Approximately 1000 measurements were collected per sample stub. The Raman system was calibrated with silicon on the 520.7 cm^{-1} line. Background measurements were automatically subtracted via the software and the corresponding mineral was identified by comparison with known spectra from the RRUFF database. The acquired spectra were each assigned a 'best fit' coefficient. This coefficient describes how well a given spectrum fits to its closest fitting spectrum from the RRUFF database and lies between 0 (a perfect fit to a spectrum in the database) and 1 (no fit to any of the spectra in the database). The higher the coefficient, the lower the certainty of grain composition. If a given grain coefficient lay between 0 and 0.15 inclusive, it was classified as a 'good hit' and was accepted. If the coefficient lay above 0.15 and at or below 0.30, the spectrum was classified as an 'OK hit', and was visually inspected, and accepted or rejected. If the coefficient for a given spectrum was over 0.30, it was rejected outright. For further details see (Lünsdorf et al., 2019).

5. Results

5.1. Light Mineral Petrography

All analysed samples fall within the feldspathic litharenite field of the QmFLt field of (Folk, 1980), with the exception of the Shwezetaw-Padaung boundary sample which plots as a litharenite (Fig. 5b). All samples have low proportions of feldspar, with medium to high amounts of monocrystalline quartz and lithic fragments. Texturally, the sandstones are highly varied. Samples from the Pondaung Formation, the lower Shwezetaw Formation, the Shwezetaw-Padaung Boundary, and the upper Padaung Formation are well sorted. The middle Shwezetaw Formation sample is moderately sorted, and samples from the upper Shwezetaw, lower Padaung and middle Padaung display poor-to-moderate degrees of sorting. The Pondaung and Shwezetaw Formation samples typically have smaller, more angular grains than the Padaung Formation samples, which have larger, often well-rounded grains. All samples plot within the 'recycled orogen' field of the QFL ternary diagram of Dickinson (1985), with the exception of the middle Padaung Formation which plots within the 'dissected arc' field (Fig. 5a). There are no clear stratigraphic grain-size trends within the light mineral petrography data.

5.2. Heavy Minerals from Raman Spectroscopy

Heavy mineral assemblages were analysed in all eight samples, seven of which yielded sufficient numbers of grains (Fig. 6). Two samples, the lower Shwezetaw Formation and the lower Padaung Formation, yielded only 29 and 100 heavy mineral grains respectively, and are omitted from discussion. ZTR (zircon-tourmaline-rutile) index ratio values were also calculated to obtain an indication of the chemical and mechanical maturity of each of the samples. A number of rare heavy minerals were obtained from each sample, and are listed as 'other' in the following sections; the minerals are listed in detail in the supplementary materials.

5.2.1. *Pondaung Formation*

The MAG_17_03 Pondaung Formation heavy mineral assemblage yielded 763 'good hit' heavy mineral grains, of which the proportions are: 34.5% epidote, 25.3% garnet, 15.6% titanite, 13.8% apatite, 3.3% chloritoid, 2.4% tourmaline, 1.4% chlorite, 0.8% zircon, 0.8% Cr-spinel, 0.3% rutile, 0.3% amphibole, and 1.7% 'other' heavy minerals (Fig. 6). This sample yielded a very small proportion of ultrastable heavy minerals, and has a ZTR ratio of 3.4%, indicating an extremely low chemical maturity. The sample has a large proportion of garnet, and also unstable heavy minerals such as epidote and titanite, which are not abundant in most other samples.

5.2.2. *Shwezetaw Formation*

Despite the lack of heavy mineral grains in the lower Shwezetaw Formation, the middle and upper Shwezetaw Formation samples (417 and 335 'good hits' respectively) yielded similar heavy mineral assemblages. The middle and upper Shwezetaw samples both possess low ZTR ratios (15.8% and 12.5% respectively), revealing significant compositional immaturity. The similarity between the two samples suggests a similar provenance.

The middle Shwezetaw Formation is characterised by the following heavy mineral proportions: 53.0% apatite, 15.4% garnet, 12.2% tourmaline, 6.0% chlorite, 3.6% zircon, 2.6% Cr-spinel, 1.7% titanite, 1.4% chloritoid, and 2.9% 'other' heavy minerals (Fig. 6). The upper Shwezetaw Formation is characterised by the following mineral proportions: 46.0% apatite, 19.1% garnet, 7.8% tourmaline, 6.6% titanite, 5.1% chlorite, 4.8% zircon, 1.8% chloritoid, 1.8% amphibole, 1.2% Cr-spinel, 0.3% epidote, and 5.7% 'other' heavy minerals (Fig. 6).

Both samples show a marked increase in apatite and tourmaline compared to the underlying Pondaung Formation, and a significant decrease in titanite, with epidote disappearing completely. In both samples, Cr-spinel is rare, indicating only a minor contribution from ophiolitic or ultramafic material.

5.2.3. *Shwezetaw-Padaung Formation Boundary Sample*

The Shwezetaw-Padaung Formation boundary sample yielded a population of 351 'good hit' heavy mineral grains, consisting of 42.7% apatite, 19.4% garnet, 14.5% tourmaline, 10.0% zircon, 8.0% Cr-spinel, 1.4% chlorite, 1.1% chloritoid, 0.6% amphibole, 0.3% rutile, and 2.0% 'other' heavy minerals (Fig. 6). The sample displays an increase in zircon and tourmaline, along with a reappearance of rutile which was absent from the preceding two samples. The sample is more mature than the previous samples, with a ZTR ratio of 24.3%. The proportion of garnet is similar to the older samples, but in contrast, titanite is completely absent, and there are smaller proportions of amphibole, chlorite, and chloritoid.

5.2.4. *Padaung Formation*

245 'good hit' heavy mineral grains were retrieved from the middle Padaung Formation. There were: 31.8% zircon, 20.8% apatite, 16.7% Cr-spinel, 15.9% tourmaline, 7.4% garnet, 2.5% rutile, 1.6% chlorite, 0.4% chloritoid, and 2.9% 'other' heavy minerals (Fig. 6). Ultrastable heavy minerals, such as zircon, tourmaline and

rutile are at their respective maximum proportions, suggesting a higher degree of maturity compared to the other samples. Garnet and apatite are both proportionally lower than in the underlying samples. However, it is notable that Cr-spinel has its maximum proportion of 16.7%.

The upper Padaung Formation sample yielded 330 'good hit' heavy mineral grains, of which 43.0% were apatite, 24.9% epidote, 12.4% garnet, 6.7% chloritoid, 5.8% tourmaline, 3.3% chlorite, 0.9% titanite, 0.6% Cr-spinel, 0.3% rutile, and 2.1% were classified as 'other' heavy minerals (Fig. 6). The sample represents a significant decrease in maturity, with an extremely low ZTR ratio of 6.1%, considerably lower than the underlying sample (middle Padaung Formation, 50.2%). Garnet returns to higher abundances that were previously seen in the Shwezetaw Formation samples. Epidote is once again a significant mineral, and Cr-spinel is below 1%.

5.3. U-Pb Detrital Zircon Geochronology

U-Pb geochronology of zircons from eight samples are presented here as no zircons were retrieved from the lower Shwezetaw sample (Fig. 7). The results are grouped by formation as zircon recovery was relatively poor for some samples, with the exception of the Padaung Formation, in which the upper sample yielded a noticeably different age population to the lower and middle samples. Cathodoluminescence images of zircon grains are shown in Fig. 8.

5.3.1. *Pondaung Formation Samples*

103 and 144 detrital zircons were analysed from MAG_17_03 and MAG_18_10 respectively. From these analyses, there were 49 and 113 concordant zircon ages

respectively, yielding a total of 162 concordant grains. The combined samples reveal a strong Late Cretaceous-Palaeogene population, with a broad Late Cretaceous peak at 60–100 Ma and a much narrower peak in the Eocene between 40-50 Ma. There are 30 Proterozoic ages, with a peak at the Palaeozoic-Neoproterozoic boundary, between 500–600 Ma. The youngest concordant zircon age is 36.8 ± 1.1 Ma, indicating a Priabonian maximum depositional age, which is in good agreement with the zircon fission track age (37.2 ± 1.2 Ma) obtained from an ash bed within the upper Pondaung Formation (Tsubamoto et al., 2002) and U-Pb zircon ages of 40.31 ± 0.65 Ma and 40.22 ± 0.86 Ma (Khin Zaw et al., 2014).

5.3.2. *Shwezetaw Formation Samples*

No detrital zircons were obtained from the lower Shwezetaw Formation, and as a result, there are no geochronological data for this sample. 124, 139, and 205 grains were analysed from the middle Shwezetaw Formation, upper Shwezetaw Formation, and Shwezetaw-Padaung Formation boundary samples, yielding 63, 76 and 166 concordant zircon ages respectively. These ages were combined into a single composite sample because of the low numbers and their broadly similar zircon age populations. This yields a total of 305 concordant grains for the Shwezetaw Formation as a whole (Fig. 7).

The combined sample shows a bimodal Late Cretaceous-Early Palaeogene population, with a strong peak between 60–70 Ma and a broader, smaller peak between 80–100 Ma. There is a significant population at the Neoproterozoic-Early Palaeozoic boundary. Subordinately, there is a substantial population of grains between 500–550 Ma in the Early Cambrian, with smaller populations spread across the Meso- and Neoproterozoic. Palaeocene grains are present, but there are no significant populations. In each of the three samples that comprise the combined sample, the youngest concordant detrital grain shows an increase in age with decreasing sample stratigraphic age; 33.4 ± 0.8 Ma, 32.1 ± 0.8 Ma, and 34.1 ± 0.8 Ma, indicating a maximum depositional age of Rupelian (Early Oligocene) for the Shwezetaw Formation.

5.3.3. *Padaung Formation Samples*

185, 180 and 47 grains were analysed from the lower Padaung Formation, middle Padaung Formation, and upper Padaung Formation samples, respectively. From these analyses, 130, 129, and 25 concordant zircon ages were retrieved respectively. The Padaung Formation samples were combined into a single composite sample because of the small number of grains and their similar age populations. This yields a total of 284 concordant grains for the Padaung Formation as a whole (Fig. 7).

The combined Padaung Formation population is mostly composed of Late Cretaceous grains, with a substantial peak between 90–100 Ma. The most notable difference between this population and the Shwezetaw Formation population is the significant reduction in Cenozoic grains. There is a subordinate Late Neoproterozoic-Cambrian population that is similar to the Shwezetaw Formation sample, and a larger Mesoproterozoic population. The youngest zircon in the combined sample is 30.8 ± 0.4 Ma, meaning the maximum depositional age of the Padaung Formation is mid-Rupelian.

6. Interpretation and Discussion

In this section, the light mineral petrography, heavy mineral assemblages, and detrital zircon geochronology are synthesised and discussed at the formation level. From these data, potential source areas and sedimentary routing pathways are discussed in the context of the regional tectonics and palaeogeography in the Oligocene, primarily based on Hall (2013, 2012), Licht et al. (2019), Westerweel et al. (2019, 2020) and Arboit et al. (2021).

6.1. Provenance Through Time

6.1.1. Priabonian Pondaung Formation

A low zircon yield appears to be a common feature of samples collected from the Pondaung Formation (Kyaw Linn Oo et al., 2015; Cai et al., 2019) and our samples are no different. Our grains show a similar overall age distribution to previous studies but they differ in the maximum depositional age. The previously reported youngest zircons are 42 Ma (Wang et al., 2014) and 43 Ma (Kyaw Linn Oo et al., 2015). Our youngest zircon (36.8 ± 1.1 Ma) is well within error of the age estimate of the ash bed (37.2 ± 1.2 Ma) reported by Tsubamoto et al. (2002) and similar to the ages reported in Khin Zaw et al. (2014), and indicates a Priabonian maximum depositional age. The considerable number of euhedral and subhedral Eocene zircons (Fig. 8) retrieved from the Pondaung Formation sample suggests input from a nearby contemporaneous igneous source during the Priabonian. Given the proximity of the Salin Sub-basin to the WPA, which had a minor active phase between 42–36 Ma (Fig. 9; Barley and Khin Zaw, 2009; Gardiner et al., 2017; Lin et al., 2019; Licht et al., 2020), we attribute these zircons to this phase of volcanism. It is possible that older sections of the arc also provided detritus at this time, indicated by a strong Late Cretaceous peak that probably reflects the 85–110 Ma peak present in the Wuntho-Popa Ranges (Fig. 9; Barley and Khin Zaw, 2009; Lin et al., 2019; Licht et al., 2020). The presence of euhedral and broken euhedral zircons (Fig. 8) around 60-70 Ma cannot be attributed to the main igneous event in the WPA and suggests input from a primary igneous source with little recycling. We propose either: 1) these zircons were sourced from a buried section of the WPA for which we currently lack geochronological data, or 2) these zircons were sourced in the MMB, which is nearby and contains intrusions which have yielded Late Cretaceous-Early Palaeogene U-Pb crystallisation ages (Fig. 9; Khin Zaw, 1990; Barley et al., 2003; Searle et al., 2007, 2020; Mitchell et al., 2012; Zhang et al., 2018; Lin et al., 2019). Previous studies show that detrital zircons in the Eocene CMB sediment have positive Hf values (Wang et al., 2014; Zhang et al., 2019; Arboit et al., 2021), whereas the intrusions in the MMB yield overwhelmingly negative Hf values (Searle et al., 2017; Gardiner et al., 2018; Lin et al., 2019); therefore, we favour the first option: a source somewhere in the buried sections of the WPA. The Gangdese Batholiths could have contributed to the Eocene zircon population, but their considerable distance from the Salin Sub-basin is inconsistent with the low heavy mineral assemblage maturity.

The presence of substantial amounts of epidote and garnet indicate a significant contribution from a metamorphic source. It is unlikely that this source is the metamorphic lithologies within the IMR for three reasons: 1) the ranges were not a significant physiogeographical feature in the Late Eocene and are likely to have been almost entirely underwater at this point (Allen et al., 2008; Licht et al., 2019; Morley et al., 2020), 2) the sample contains minor amounts (<1%) of Cr-spinel, a typical indicator of ophiolitic material, which is abundant in the Western Ophiolite Belt of the IMR

(Soibam et al., 2015; Hla Htay et al., 2017), and 3) the regionally-extensive Pane Chaung Formation of the IMR basement contains distinctively strong Triassic and Neoproterozoic zircon age populations (Fig. 9; Sevastjanova et al., 2016; Yao et al., 2017) which are non-existent (in the case of the Triassic signal) or indistinct (in the case of the Neoproterozoic signal) in our Pondaung Formation samples (Fig. 7, 9), suggesting minimal input from the metamorphic lithologies in the IMR. The MMB could be a source for the metamorphic heavy minerals we have found, given the multitudes of medium-high grade metamorphic rocks in the area which contain garnet and epidote (review in Searle et al., 2017), and the Cretaceous-Palaeogene ages of its intrusions. However, given that previous studies (Wang et al., 2014; Zhang et al., 2019; Arboit et al., 2021) have found negative Hf values in the MMB and positive Hf values in the Eocene strata of the CMB, we suggest that a different metamorphic source is responsible for the contribution of epidote and garnet, and their abundance indicates that this source was probably proximal. Limited palaeocurrent indicators from the Pondaung Formation indicate flow was predominantly to the southwest (Licht et al., 2013), further suggesting that this source was located to the north or northeast of the Salin Sub-basin. Metamorphic regions to the north/northeast that are relatively proximal include the basement metamorphic regions surrounding the Jade Mines Belt. The lack of a strong Early Cretaceous zircon age signal further suggests input from the Western Ophiolite Belt was negligible, so the Cr-spinel in this sample is probably derived from the Eastern Ophiolite Belt. We therefore propose that much of the detrital metamorphic material in the Pondaung Formation is derived from the basement rocks of northern Myanmar.

Overall, the Pondaung Formation has a mixed provenance, with input from a northern metamorphic source, possibly the metamorphic basement rocks of northern Myanmar, and a substantial contribution from an active—or recently active—igneous source, which we interpret to be the now partially-buried WPA (Fig. 10). It is possible that the MMB also provided sediment, but without Hf data, we cannot confirm this. A contribution of sediment from the Dianxi batholith in south China or Gangdese Batholiths in the Himalayas are other plausible explanations for the Late Cretaceous and Eocene zircon populations but these sources are too far away from CMB to account for the low ZTR ratios in the heavy mineral population.

6.1.2. *Rupelian Shwezetaw Formation*

The relative decrease in Cenozoic zircons and increase in Late Cretaceous zircons in the Shwezetaw Formation compared to the Pondaung Formation could be attributed to a decrease in input from the younger areas of the WPA, and a concurrent increase in input from older sections of the arc, such as the 86–106 Ma signal observed in the northern regions of the Wuntho Ranges (Fig. 9; e.g. Licht et al., 2020). Alternatively, this peak could be attributed to input from the Chin Hills region of the IMR, which has a strong 80–100 Ma population (Fig. 9, Sevastjanova et al., 2016). Our 80–100 Ma zircons are mostly subhedral to subrounded in form, suggesting they are polycyclic, and were not derived directly from the WPA; a few grains of this age are euhedral, suggesting they originated directly from an igneous source. Both the subhedral-subrounded and euhedral grains of this age show simple oscillatory zoning, suggesting that they were both originally from an igneous source. We interpret this population of zircons to be primarily derived from the Cretaceous sedimentary rocks in the Chin Hills region (Fig. 7), which contains zircons originally derived from the

WPA. Subordinately, the WPA also provided primary igneous material directly to the Salin Sub-basin, evidenced by the presence of euhedral zircons.

As in older samples, the significant population of 50–70 Ma zircons is not directly attributable to the WPA or the Chin Hills, so the source for this population remains unclear. Their forms are often euhedral suggesting minimal amounts of reworking. Like the Pondaung Formation, one possibility is that they were sourced by Late Cretaceous-Early Palaeogene WPA volcanics that were subsequently buried by the Neogene sediments of the CMB (Licht et al., 2013; Zhang et al., 2017). The Sodon Batholith and pre-Eocene sedimentary strata have zircons with crystallisation and detrital ages respectively that suggest the WPA was sporadically active between ~50 and ~70 Ma (Fig. 9, Zhang et al., 2017; Lin et al., 2019). Alternatively, many of the batholiths which intrude the metasedimentary rocks of the MMB, have U-Pb crystallisation ages of between 50 and 70 Ma (Fig. 9; Mitchell et al., 2012; Xie et al., 2016; Mitchell, 2017; Li et al., 2019; Lin et al., 2019), so could have been a source at this time. Local palaeogeographic reconstructions in Licht et al. (2019) show the transport of sediment from the MMB to the forearc trough of the CMB starting in the Oligocene, and this is also suggested to be a source for the CMB in Arboit et al. (2021). Both of these models show the MMB extending along the entire eastern flank of the CMB in the mid-Oligocene, and if this is the case, the granitoid intrusions and the metamorphic lithologies in the MMB are highly plausible sources for the 50–70 Ma zircons and metamorphic minerals. A similar regional palaeotectonic reconstruction in Westerweel et al. (2020) also shows transport of sediment occurring westwards across the WPA, although this model shows the MMB to be approximately 2000 km to the north of the Salin Sub-basin in the Eocene. If this model is correct, the compositional immaturity of the Shwezetaw Formation heavy mineral population is incompatible with such a distal source.

The Late Neoproterozoic-Early Cambrian peak at ~550 Ma and subordinate Mesoproterozoic population are typical of 'Gondwanan/Pan-African' signals present in Palaeozoic and Mesozoic Sibumasu Terrane metasedimentary rocks (Hall and Sevastjanova, 2012). However, the sample also contains a minor Triassic signal, which, at its peak, is approximately 25% of the strength of the Late Neoproterozoic-Early Cambrian signal. This is a key characteristic of zircons from the Pane Chaung Formation (Fig. 9; Sevastjanova et al., 2016) in the IMR. Zircon grains of this age in our samples are highly rounded (Fig. 8), suggesting that they are polycyclic and were potentially reworked from such sedimentary deposits.

This Pane Chuang Formation signal, along with the Chin Hills signal, is clear evidence that the IMR were topographically significant enough to provide sediment from the inner wedge in the Early Oligocene. This also implies that the Kanpetlet Schists (also part of the inner wedge of the IMR) could have provided metamorphic detritus at this time.

Cr-spinel, a mineral commonly found in ultramafic and ophiolitic lithologies, increases in abundance with decreasing sample age in the Shwezetaw Formation, reaching 7.9% in the Shwezetaw-Padaung Formation boundary sample (Fig. 6). The compositional immaturity of the heavy mineral assemblages suggests a relatively local source; this implies that a proximal ultramafic or ophiolitic source was providing sediment to the Salin Sub-basin in the earliest Oligocene. Given that much of the

Eocene and Oligocene sediment in the Salin Sub-basin records south to southwest trending palaeoflows (Licht et al., 2013; Gough et al., 2020), it is likely that this proximal ultramafic or ophiolitic source was to the north or north-east. There are therefore two possible sources for the Cr-spinel: 1) the northern sections of the Western Ophiolite Belt, and 2) the Eastern Ophiolite Belt.

The northern region of the IMR, which underwent incipient uplift in the early Oligocene (Mitchell, 2017; Licht et al., 2019; Gough et al., 2020; Morley et al., 2020; Najman et al., 2020) prior to the uplift of the southern ranges (Westerweel et al., 2020), could have contributed ophiolite-derived sediment to the Salin Sub-basin. In this case, the increasing proportions of Cr-spinel in the Shwezetaw Formation may have derived from the discontinuous outcrops of the Western Ophiolite Belt and could document the progressive uplift of the inner wedge of the IMR to the north of the Salin Sub-basin. However, as was the case in the Pondaung Formation, the lack of significant amounts of 110–130 Ma zircons precludes this and suggests that the Western Ophiolite Belt was not providing enough sediment at this time to account for the Cr-spinel signal by itself.

Alternatively, or additionally, the Jade Belt—part of the Eastern Ophiolite Belt—may be the source. The Jade Belt in northern Myanmar is composed of serpentinized peridotites as well as widespread schist and amphibolite-grade metamorphics (Shi et al., 2001). Garnet, zircon, Cr-spinel, chlorite and titanite are all present within the Jade Belt and its associated lithologies (Shi et al., 2012). Glaucophane, an accessory mineral present in all of the Shwezetaw Formation samples, is also found in Na-rich, Cr-dominant lithologies in the Jade Belt (Shi et al., 2012). Grossular is by far the most common garnet-group mineral that occurs in the Jade Belt schists (Shi et al., 2012). Raman spectroscopy alone does not allow for definitive identification of specific endmembers of minerals in solid solution, however, the majority of garnets in the middle and upper Shwezetaw Formation samples matched most closely with spectra produced by grossular. In future studies, there is scope to check speciation of these detrital garnets, which may be able to help better understand the source. The common U-Pb ages of 163.2 ± 3.3 Ma and 146.5 ± 3.4 Ma that are common in zircons from the Jade Belt (Shi et al., 2008) are not prominent in the Shwezetaw samples (Fig. 7). Given that both the Western and Eastern Ophiolite Belts contain populations of Jurassic to Cretaceous zircons that are not present in our samples in any significant number (Fig. 7), we suggest that the Cr-spinel signal could be derived from a contribution from both regions.

The striking similarities between the heavy mineral assemblages of the middle Shwezetaw Formation, upper Shwezetaw Formation, and the Shwezetaw-Padaung Formation boundary samples suggest that a stable mixed provenance regime prevailed throughout the deposition of the formations. We conclude that the source regions of the Shwezetaw Formation are difficult to determine exactly, although the sedimentary routing pathway is likely to have had headwaters in both the basement of the IMR, which provided metamorphic material and recycled zircons from the Pane Chuang Formation, and in northern Myanmar (Fig. 10). The northern pathway likely had a catchment in the Jade Mines Belt. Downstream, tributaries provided material shed from the WPA, which provided much of the Cretaceous-Palaeogene zircons along with the MMB (Fig. 11). We cannot ascertain if the MMB was providing sediment at this time.

6.1.3. Rupelian Padaung Formation

The Padaung Formation records a subtle shift in provenance, shown by a proportional increase of the 90–100 Ma zircon population, and a coeval decrease in the Cenozoic zircon populations compared to the underlying formations. The main zircon population peak between 90 and 100 Ma aligns with zircon crystallisation ages from the Wuntho Ranges rivers and the WPA (Fig. 9; Gardiner et al., 2017; Li et al., 2019; Lin et al., 2019; Licht et al., 2020), but once again, also aligns well with U-Pb ages from the Chin Hills (Fig. 9; Sevastjanova et al., 2016). In our Padaung Formation samples, grains of this age have similar morphologies to those in the Shwezetaw Formation samples; they are typically subhedral or subrounded (Fig. 8), which suggests polycyclicity. These morphologies indicate that the 80–100 Ma population were derived from the Chin Hills, and their age and simple oscillatory zoning is suggestive of an original provenance in the WPA. We propose that the dominant Late Cretaceous peak is evidence of provenance in the Chin Hills, which provided recycled WPA material to the Salin Sub-basin. This also explains the lack of the 36–42 Ma population observed in the WPA–the youngest zircon in the Chin Hills marlstone dataset is ~81 Ma, so the Chin Hills sediments cannot have captured the younger igneous event in the WPA. The similarities of the ratios between the Proterozoic and Triassic zircon age populations in both the Shwezetaw and Padaung Formation samples suggest that the Pane Chuang Formation continued to provide material to the CMB in the Rupelian (Fig. 9).

The reduced 50–70 Ma zircon population in the Shwezetaw Formation compared to older samples suggests reduced input from the MMB or WPA (Fig. 9). If these zircons are MMB-derived, then this could be attributed to the partitioning of the sub-basins which began at 39–38 Ma (Licht et al., 2019), effectively shutting down the transport of material from the MMB eastwards across the backarc basins to the Salin Sub-basin. Alternatively, if they are WPA-derived, this could indicate burial of the section of the arc which provided Late Cretaceous-Early Palaeogene grains.

In the middle Padaung Formation, there is a substantial amount of material from igneous lithologies indicated by the large number of primary igneous minerals such as zircon, tourmaline and apatite (Fig. 6). The large amount of Cr-spinel indicates concurrent input from local topographic highs of ophiolitic and ultramafic lithologies in the IMR, and upstream from the ophiolites in the Eastern Ophiolite Belt. The heavy mineral assemblage of the upper Padaung Formation starkly contrasts that of the middle Padaung Formation (Fig. 6), suggesting a change in provenance which is emphasised by the decrease of primary igneous minerals and chemical maturity, and the concurrent increase in medium-grade metamorphic minerals. The mid-Oligocene uplift in the IMR suggested in Najman et al. (2020) could account for this large increase in medium-grade metamorphic material from the basement of the inner wedge of the ranges.

The varied heavy mineral assemblages of the Padaung Formation samples are indicative of a variety of diverse lithologies acting as sources at this time, in marked contrast to the more stable sources of the Shwezetaw Formation. The timing of the switch to a more diverse provenance appears to have occurred after or during deposition of the middle Padaung Formation, owing to the vastly different heavy mineral assemblage in the upper Padaung Formation (Fig. 6).

6.2. Source Areas and Routing Pathways

It is clear from the combined detrital zircon geochronology and heavy mineral data that the primary source areas were primarily igneous and metamorphic (although some recycled sedimentary material is also present), and that these sources varied in the amount of sediment they provided to the Salin Sub-basin throughout the deposition of the Pondaung, Shwezetaw and Padaung Formations. We identify four primary sources: 1) the WPA, 2) the IMR, 3) the MMB, and 4) Northern Myanmar (including the Eastern Ophiolite Belt and Jade Mines Belt). Our proposed model for each formation is depicted in Fig. 10 and shows the evolution of the sedimentary pathway configuration in the CMB throughout the deposition of the studied formations. Our wider-scale interpretation of the sedimentary routing pathway is shown in Fig. 11.

The WPA provided sediment to the Salin Sub-basin throughout the deposition of the studied formations, both directly and indirectly. Contemporaneous sections of the arc provided igneous material in the Eocene, and both the WPA and Chin Hills provided primary arc material and recycled arc material respectively in the Oligocene (Fig. 10).

Both the Shwezetaw and Padaung Formations record evidence of input from recycled Sibumasu material in their Precambrian detrital zircon populations, which we attribute to input from the Pane Chuang Formation. The Chin Hills also provided material throughout deposition of these formations. The Padaung Formation records a particularly strong signal from the sedimentary rocks of the Chin Hills, indicating that further uplift of the IMR to the northwest of the Salin Sub-basin must have taken place during the Oligocene, and that this was an important sediment source for the basin.

The IMR are suggested to have uplifted in two main phases: an initial Palaeogene phase in which the northern inner wedge uplifted during the late Eocene and early Oligocene and the main inner wedge uplifted in the mid-Oligocene, and a secondary Neogene phase where the outer wedge uplifted in the Miocene-Pliocene (Licht et al., 2019). The increase in Chin Hills zircons in our Oligocene samples could be attributed to the mid-Oligocene phase of uplift proposed in Najman et al. (2020). We suggest that much of the sedimentary detritus in the Oligocene formations sampled in this study could be at least partially derived from the inner wedge of the IMR. The Pondaung Formation does contain a similar Proterozoic signal but given the lower number of zircons grains and lack of a strong Triassic signal, we cannot attribute this to the Pane Chuang Formation, and therefore cannot confirm if any nascent, isolated uplifts of the IMR were providing sediment to the Salin Sub-basin in the latest Eocene.

The intrusions in the MMB are plausible sources for the 50-70 Ma population of zircons that cannot be directly accounted for in the WPA. However, the model of Westerweel et al. (2020) precludes eastward transport across the backarc basin owing to the presence of a substantial body of water to the east of the backarc basin. The palaeogeographic and palaeotectonic reconstructions in Licht et al. (2019), Morley et al. (2020) and Arboit et al. (2021) do not include this body of water and show juxtaposition of the MMB with the eastern edge of the CMB, and our data is compatible with these models. This population of zircons could also be sourced in a presently buried section of the WPA to the north, but without Hf data to indicate the provenance of these grains, we cannot be certain of this.

The Jade Mines Belt/Eastern Ophiolite Belt in northern Myanmar is a possible source for the large amounts of detrital metamorphic and ophiolite-derived heavy minerals in our samples, owing to its northern location, proximity to the WPA, Cretaceous-to-Eocene age (see reviews in Searle et al., 2017), and large exposures of medium-high grade metamorphic lithologies and ultramafic material. This may be the source of much of the Cr-spinel in our samples, although it is difficult to constrain the amount of material that was also shed from the Western Ophiolite Belt in the IMR to the CMB. Cr-spinel is commonly found in the peridotites of the Western Ophiolite Belt in the northern IMR (Singh, 2009, 2013), as well as in the Eastern Ophiolite Belt in the Jade Mines and Myitkyina regions (Shi et al., 2012), so our Cr-spinel signal could have originated from either locality. Both ophiolite belts are associated with Triassic Pane Chuang Formation and Kanpetlet Schist, and their equivalents. The large proportions of Cr-spinel seen at the Shwezetaw-Padaung Formation boundary and in the middle Padaung Formation could be attributed to increased input from either the Western or Eastern Ophiolite Belts.

In the late Eocene, during deposition of the Pondaung Formation, sediment was derived primarily from a northern metamorphic source, which we interpret as the metamorphic basement lithologies in northern Myanmar, including the Jade Mines Belt and Eastern Ophiolite Belt which provided ophiolitic material (Fig. 10). At this time, tributaries also drained the recent volcanics of the WPA. In the Early Oligocene during deposition of the Shwezetaw Formation (Fig. 11), there was a stable provenance regime with sediment primarily transported proximally from the IMR. Sediment was also derived from northern Myanmar including the Jade Mines Belt and Eastern Ophiolite Belt. Increasing amounts of Cr-spinel suggests increasing input from either the IMR or northern Myanmar throughout deposition of the formation but given that the IMR are suggested to have undergone uplift at this time, we propose that most of the Cr-spinel was derived from the proximal Western Ophiolite Belt. The MMB could also have provided sediment at this time, either southwards from the north or eastwards across the backarc basins (as in Licht et al., 2019); alternatively, currently buried sections of the WPA could be a source. During deposition of the Padaung Formation, the IMR continued to provide sediment to the CMB. The concurrent reduction in 50–70 Ma zircons suggests that input from the MMB or WPA was declining, either because of further partitioning of the forearc-backarc couplet (in the case of the MMB) or burial of the section of the arc providing these grains (in the case of the WPA).

7. Conclusions

1. The inner wedge of the Indo-Myanmar Ranges was a significant geographic feature by the mid-Oligocene and was an important source of sediment for the Salin Sub-basin during deposition of the Shwezetaw and Padaung Formations. The Chin Hills region provided polycyclic igneous material originally derived from the Late Cretaceous igneous phase of the nearby Wuntho-Popa Arc. The Triassic Pane Chuang Formation was also a persistent source, characterised by the consistent Triassic-Neoproterozoic zircon population ratios observed in the two Oligocene formations.
2. The Wuntho-Popa Arc directly provided various amounts of igneous material to the Salin Sub-basin throughout deposition of the studied formations. The Pondaung Formation records strong evidence of contemporaneous volcanism in the Eocene Wuntho-Popa Arc, whereas the Shwezetaw and Padaung Formations record significantly reduced activity in the Oligocene. During these

times the arc was still a source but contributed less sediment than in the Eocene.

3. The source of the 50–70 Ma zircon grain population remains unclear; however, these zircons could represent input from the intrusions in the Mogok Metamorphic Belt, either from the north (in which case it is plausible that it shares the same routing pathways as the signal from northern Myanmar), or eastwards across the backarc trough of the Central Myanmar Basin. In any case, this signal appears to reduce in the Padaung Formation, suggesting either: 1) a switch in provenance away from the Mogok Metamorphic Belt in northern Myanmar, or 2) cessation of the eastward transport of material from across the backarc basin. Alternatively, this population of zircons may be derived from an area of the Wuntho-Popa Arc that is currently buried, and for which we have no age data; in this case, the reduction of the signal may be due to progressive burial of the arc in this location.
4. The ubiquitous presence of metamorphic-derived heavy mineral grains suggests input from any or all of the following: 1) the Kanpetlet Schists (Indo-Myanmar Ranges basement), 2) Northern Myanmar (including the Jade Mines Belt and Eastern Ophiolite Belt), and 3) the Mogok Metamorphic Belt.

Declaration of Competing Interest

The authors declare that they have no known competing financial interests or personal relationships that could have appeared to influence the work reported in this paper.

Data

Supplementary information including datasets and additional files for this research are available at https://doi.org/10.6084/m9.figshare.14346836. The data includes:

- Tabulated heavy mineral proportions, as well as information on the accessory heavy minerals.
- Tabulated U-Pb detrital zircon ages for each sample.
- A compilation of published U-Pb data used for comparisons in this study.

Acknowledgements

This research was funded by the SE Asia Research Group at Royal Holloway, supported by a consortium of oil companies. We thank ENI for support during fieldwork, and invaluable feedback on the work. We also thank Neil Holloway for the production of thin sections, Professor Andrew Carter of the London Geochronology Centre for assistance with LA-ICP-MS analysis, and the staff at the Department of Sedimentology and Environmental Geology, University of Göttingen, for their assistance with Raman spectroscopy. Thanks also goes to Dr Christina Manning for her assistance with LA-ICP-MS analysis at Royal Holloway, University of London. Two reviewers, Dr Alexis Licht and Dr Jan Westerweel, and the editor, Professor Khin Zaw, are thanked for their insightful comments, suggestions, and questions, which were instrumental in the production of the final manuscript.

References

Allen, R., Najman, Y., Carter, A., Barfod, D., Bickle, M.J., Chapman, H.J., Garzanti, E., Vezzoli, G., Andò, S., Parrish, R.R., 2008. Provenance of the Tertiary sedimentary rocks of the Indo-Burman Ranges, Burma (Myanmar): Burman arc or Himalayan-derived? Journal of the Geological Society 165, 1045–1057. https://doi.org/10.1144/0016-76492007-143

Arboit, F., Min, M., Chew, D., Mitchell, A., Drost, K., Badenszki, E., Daly, J.S., 2021. Constraining the links between the Himalayan belt and the Central Myanmar Basins during the Cenozoic: An integrated multi-proxy detrital geochronology and trace-element geochemistry study. Geoscience Frontiers 12, 657–676. https://doi.org/10.1016/j.gsf.2020.05.024

Aung Naing Soe, Myitta, Tun, S.T., Aung, A.K., Thein, T., Marandat, B., Ducrocq, S., Jaeger, J.-J., 2002. Sedimentary facies of the late Middle Eocene Pondaung Formation (central Myanmar) and the palaeoenvironments of its Anthropoid Primates. Comptes Rendus Palevol 1, 153–160. https://doi.org/10.1016/S1631-0683(02)00020-9

Aye Ko Aung, 2004. The Primate-Bearing Pondaung Formation in the Upland Area, Northwest of Central Myanmar, in: Ross, C.F., Kay, R.F. (Eds.), Anthropoid Origins: New Visions. Springer US, Boston, MA, pp. 205–217. https://doi.org/10.1007/978-1-4419-8873-7_9

Bannert, D., Sang Lyen, A., Htay, T., 2011. The Geology of the Indoburman ranges in Myanmar: with 3 tables, Geologisches Jahrbuch Reihe B, Regionale Geologie Ausland. Schweizerbart, Stuttgart.

Barley, M.E., Pickard, A.L., Khin Zaw, Rak, P., Doyle, M.G., 2003. Jurassic to Miocene magmatism and metamorphism in the Mogok metamorphic belt and the India-Eurasia collision in Myanmar: MAGMATISM AND METAMORPHISM IN THE MOGOK BELT, MYANMAR. Tectonics 22, n/a-n/a. https://doi.org/10.1029/2002TC001398

Barley, M.E., Khin Zaw, 2009. SHRIMP U-Pb in zircon geochronology of granitoids from Myanmar: temporal constraints on the tectonic evolution of Southeast Asia, in: EGU General Assembly Conference Abstracts, EGU General Assembly Conference Abstracts. p. 3842.

Beard, K.C., Marivaux, L., Chaimanee, Y., Jaeger, J.-J., Marandat, B., Tafforeau, P., Soe, A.N., Tun, S.T., Kyaw, A.A., 2009. A new primate from the Eocene Pondaung Formation of Myanmar and the monophyly of Burmese amphipithecids. Proc. R. Soc. B. 276, 3285–3294. https://doi.org/10.1098/rspb.2009.0836

Bender, F., 1983. Geology of Burma. Schweizerbart Science Publishers, Stuttgart, Germany.

Bertrand, G., Rangin, C., 2003. Tectonics of the western margin of the Shan plateau (central Myanmar): Implication for the India-Indochin oblique convergence since the Oligocene. Journal of Asian Earth Sciences 21, 1139–1157. https://doi.org/10.1016/S1367-9120(02)00183-9

Betka, P.M., Seeber, L., Thomson, S.N., Steckler, M.S., Sincavage, R., Zoramthara, C., 2018. Slip-partitioning above a shallow, weak décollement beneath the Indo-Burman accretionary prism. Earth and Planetary Science Letters 503, 17–28. https://doi.org/10.1016/j.epsl.2018.09.003

Brunnschweiler, R.O., 1966. On the geology of the Indoburman ranges: (Arakan Coast and Yoma, Chin Hills, Naga Hills). Journal of the Geological Society of Australia 13, 137–194. https://doi.org/10.1080/00167616608728608

Cai, F., Ding, L., Zhang, Q., Orme, D.A., Wei, H., Li, J., Zhang, J., Zaw, T., Sein, K., 2019. Initiation and evolution of forearc basins in the Central Myanmar Depression. Geological Society of America Bulletin 132, 17.

Chaimanee, Y., Chavasseau, O., Beard, K.C., Kyaw, A.A., Soe, A.N., Sein, C., Lazzari, V., Marivaux, L., Marandat, B., Swe, M., Rugbumrung, M., Lwin, T., Valentin, X., Zin-Maung-Maung-Thein, Jaeger, J.-J., 2012. Late Middle Eocene primate from Myanmar and the initial anthropoid colonization of Africa. Proceedings of the National Academy of Sciences 109, 10293–10297. https://doi.org/10.1073/pnas.1200644109

Chhibber, H.L., 1934. The geology of Burma. Macmillan and Company, limited.

Ciochon, R.L., Holroyd, P.A., 1994. The Asian Origin of Anthropoidea Revisited, in: Fleagle, J.G., Kay, R.F. (Eds.), Anthropoid Origins. Springer US, Boston, MA, pp. 143–162. https://doi.org/10.1007/978-1-4757-9197-6_6

Clegg, E.L.G., 1938. The geology of parts of the Minbu and Thayetmyo Districts, Burma. Geological Survey of India.

Curray, J.R., 1989. The Sunda Arc: A Model For Oblique Plate Convergence 24, 131–140.

Day Wa Aung, 2012. Sedimentology of Oligocene clastic strata in the western part of the Minbu Basin, Myanmar, in: GeoMyanmar 2012. Presented at the First International Conference on Myanmar Geology.

Dickinson, W., 1985. Interpreting Provenance Relations from Detrital Modes of Sandstones, in: Provenance Arenites. pp. 333–361. https://doi.org/10.1007/978-94-017-2809-6_15

Eames, F.E., 1950. On the Ages of Certain Upper Tertiary Beds of Peninsular India and Ceylon. Geological Magazine 87, 233–252. https://doi.org/10.1017/S0016756800077049

Folk, R.L., 1980. Petrology of Sedimentary Rocks. Hemphll Publishing Company, Austin 170. https://doi.org/10.1017/CBO9781107415324.004

Galin, T., Breitfeld, H.T., Hall, R., Sevastjanova, I., 2017. Provenance of the Cretaceous–Eocene Rajang Group submarine fan, Sarawak, Malaysia from light and heavy mineral assemblages and U-Pb zircon geochronology. Gondwana Research 51, 209–233. https://doi.org/10.1016/j.gr.2017.07.016

Gardiner, N.J., Hawkesworth, C.J., Robb, L.J., Whitehouse, M.J., Roberts, N.M.W., Kirkland, C.L., Evans, N.J., 2017. Contrasting Granite Metallogeny through the Zircon Record: A Case Study from Myanmar. Sci Rep 7, 748. https://doi.org/10.1038/s41598-017-00832-2

Gardiner, N.J., Searle, M.P., Morley, C.K., Robb, L.J., Whitehouse, M.J., Roberts, N.M.W., Kirkland, C.L., Spencer, C.J., 2018. The crustal architecture of Myanmar imaged through zircon U-Pb, Lu-Hf and O isotopes: Tectonic and metallogenic implications. Gondwana Research 62, 27–60. https://doi.org/10.1016/j.gr.2018.02.008

Garzanti, E., Wang, J.G., Vezzoli, G., Limonta, M., 2016. Tracing provenance and sediment fluxes in the Irrawaddy River basin (Myanmar). Chemical Geology 440, 73–90. https://doi.org/10.1016/j.chemgeo.2016.06.010

Ghose, N.C., Chatterjee, N., Fareeduddin, 2014. A Petrographic Atlas of Ophiolite: An example from the eastern India-Asia collision zone, 1st ed. 2014. ed. Springer India : Imprint: Springer, New Delhi. https://doi.org/10.1007/978-81-322-1569-1

Gough, A., Hall, R., BouDagher-Fadel, M.K., 2020. Mid-Cenozoic fluvio-deltaic to marine environments of the Salin Sub-basin, Central Myanmar. Journal of

Asian Earth Sciences 190, 104143. https://doi.org/10.1016/j.jseaes.2019.104143

Griffin, W., Powell, W., Pearson, N.J., O'Reilly, S., 2008. GLITTER: data reduction software for laser ablation ICP-MS. Short Course Series 40, 308–311.

Hall, R., 2002. Cenozoic geological and plate tectonic evolution of SE Asia and the SW Pacific: Computer-based reconstructions, model and animations. Journal of Asian Earth Sciences 20, 353–431. https://doi.org/10.1016/S1367-9120(01)00069-4

Hall, R., 2012. Late Jurassic-Cenozoic reconstructions of the Indonesian region and the Indian Ocean. Tectonophysics 570–571, 1–41. https://doi.org/10.1016/j.tecto.2012.04.021

Hall, R., 2013. The palaeogeography of Sundaland and Wallacea since the Late Jurassic. Journal of Limnology 72, 1–17. https://doi.org/10.4081/jlimnol.2013.s2.e1

Hall, R., Morley, C.K., 2004. Sundaland basins. Geophysical Monograph Series 149, 55–85. https://doi.org/10.1029/149GM04

Hall, R., Sevastjanova, I., 2012. Australian crust in Indonesia. Australian Journal of Earth Sciences 59, 827–844. https://doi.org/10.1080/08120099.2012.692335

Hennig, J., Im Breitfeld, H.T., Gough, A., Hall, R., Van Long, T., Kim, V.M., Quang, S.D., 2018. U-PB zircon ages and provenance of upper cenozoic sediments from the da lat zone, se Vietnam: Implications for an intra-miocene unconformity and paleo-drainage of the proto-mekong river. Journal of Sedimentary Research 88, 495–515. https://doi.org/10.2110/jsr.2018.26

Hla Htay, Khin Zaw, Than Oo, 2017. Chapter 6 The mafic–ultramafic (ophiolitic) rocks of Myanmar. Geological Society, London, Memoirs 48, 117–141. https://doi.org/10.1144/M48.6

Hla Mon, 1999. Nannopaleontological analysis of the rock samples collected by the Pondaung Fossils Expedition Team. Presented at the Proceedings of the Pondaung Fossil Expedition Team, Office of Strategic Studies, Ministry of Defence.

Hutchison, C.S., 1989. Geological evolution of South-east Asia. Clarendon Press ; Oxford University Press, Oxford; New York.

Jaeger, J.-J., Thein, T., Benammi, M., Chaimanee, Y., Soe, A.N., Lwin, T., Tun, T., Wai, S., Ducrocq, S., 1999. A New Primate from the Middle Eocene of Myanmar and the Asian Early Origin of Anthropoids. Science 286, 528–530. https://doi.org/10.1126/science.286.5439.528

Khin Zaw, 1990. Geological, petrogical and geochemical characteristics of granitoid rocks in Burma: with special reference to the associated W□Sn mineralization and their tectonic setting. Journal of Southeast Asian Earth Sciences 4, 293–335. https://doi.org/10.1016/0743-9547(90)90004-W

Khin Zaw, Meffre, S., Takai, M., Suzuki, H., Burrett, C., Thaung Htike, Zin Maung Maung Thein, Tsubamoto, T., Egi, N., Maung Maung, 2014. The oldest anthropoid primates in SE Asia: Evidence from LA-ICP-MS U–Pb zircon age in the Late Middle Eocene Pondaung Formation, Myanmar. Gondwana Research 26, 122–131. https://doi.org/10.1016/j.gr.2013.04.007

Kyaw Linn Oo, Khin Zaw, Meffre, S., Myitta, Day Wa Aung, Lai, C.-K., 2015. Provenance of the Eocene sandstones in the southern Chindwin Basin, Myanmar: Implications for the unroofing history of the Cretaceous–Eocene magmatic arc. Journal of Asian Earth Sciences 107, 172–194. https://doi.org/10.1016/j.jseaes.2015.04.029

Li, J.-X., Fan, W.-M., Zhang, L.-Y., Evans, N.J., Sun, Y.-L., Ding, L., Guan, Q.-Y., Peng, T.-P., Cai, F.-L., Sein, K., 2019. Geochronology, geochemistry and Sr–Nd–Hf isotopic compositions of Late Cretaceous–Eocene granites in southern Myanmar: Petrogenetic, tectonic and metallogenic implications. Ore Geology Reviews 112, 103031. https://doi.org/10.1016/j.oregeorev.2019.103031

Licht, A., France-Lanord, C., Reisberg, L., Fontaine, C., Soe, A.N., Jaeger, J.-J., 2013. A palaeo Tibet–Myanmar connection? Reconstructing the Late Eocene drainage system of central Myanmar using a multi-proxy approach. Journal of the Geological Society 170, 929–939. https://doi.org/10.1144/jgs2012-126

Licht, A., Boura, A., De Franceschi, D., Ducrocq, S., Aung Naing Soe, Jaeger, J.-J., 2014a. Fossil woods from the late middle Eocene Pondaung Formation, Myanmar. Review of Palaeobotany and Palynology 202, 29–46. https://doi.org/10.1016/j.revpalbo.2013.12.002

Licht, A., Cojan, I., Caner, L., Soe, A.N., Jaeger, J.-J., France-Lanord, C., 2014b. Role of permeability barriers in alluvial hydromorphic palaeosols: The Eocene Pondaung Formation, Myanmar. Sedimentology 61, 362–382. https://doi.org/10.1111/sed.12059

Licht, A., Reisberg, L., France-Lanord, C., Naing Soe, A., Jaeger, J.-J., 2014c. Cenozoic evolution of the central Myanmar drainage system: insights from sediment provenance in the Minbu Sub-Basin. Basin Res 28, 237–251. https://doi.org/10.1111/bre.12108

Licht, A., Dupont-Nivet, G., Win, Z., Swe, H.H., Kaythi, M., Roperch, P., Ugrai, T., Littell, V., Park, D., Westerweel, J., Jones, D., Poblete, F., Aung, D.W., Huang, H., Hoorn, C., Sein, K., 2019. Paleogene evolution of the Burmese forearc basin and implications for the history of India-Asia convergence. GSA Bulletin 131, 730–748. https://doi.org/10.1130/B35002.1

Licht, A., Win, Z., Westerweel, J., Cogné, N., Morley, C.K., Chantraprasert, S., Poblete, F., Ugrai, T., Nelson, B., Aung, D.W., Dupont-Nivet, G., 2020. Magmatic history of central Myanmar and implications for the evolution of the Burma Terrane. Gondwana Research 87, 303–319. https://doi.org/10.1016/j.gr.2020.06.016

Lin, T.H., Mitchell, A.H.G., Chung, S.-L., Tan, X.-B., Tang, J.-T., Oo, T., Wu, F.-Y., 2019. Two parallel magmatic belts with contrasting isotopic characteristics from southern Tibet to Myanmar: zircon U–Pb and Hf isotopic constraints. Journal of the Geological Society 176, 574–587. https://doi.org/10.1144/jgs2018-072

Lünsdorf, N.K., Kalies, J., Ahlers, P., Eynatten, H. Von, 2019. Semi-Automated Heavy-Mineral Analysis by Raman Spectroscopy. Minerals 9, 32.

Ma, L., Wang, Y., Fan, W., Geng, H., Cai, Y., Zhong, H., Liu, H., Xing, X., 2014. Petrogenesis of the early Eocene I-type granites in west Yingjiang (SW Yunnan) and its implication for the eastern extension of the Gangdese batholiths. Gondwana Research 25, 401–419. https://doi.org/10.1016/j.gr.2013.04.010

Maibam, B., Foley, S., Luguet, A., Jacob, D.E., Singh, T.B., Ray, D., Panda, D.K., Keppler, R., 2017. Characterisation of chromites, chromite hosted inclusions of silicates and metal alloys in chromitites from the Indo-Myanmar ophiolite belt of Northeastern India. Ore Geology Reviews 90, 260–273. https://doi.org/10.1016/j.oregeorev.2017.05.032

Mange, M., Idleman, B., Yin, Q.-Z., Hidaka, H., Dewey, J., 2010. Detrital heavy minerals, white mica and zircon geochronology in the Ordovician South Mayo

Trough, western Ireland: signatures of the Laurentian basement and the Grampian orogeny. Journal of the Geological Society 167, 1147–1160. https://doi.org/10.1144/0016-76492009-091

Maung, K., 1970. Biostratigraphy of the Central Burma with special reference to the depositional conditions during Late Oligocene and Early Miocene. Union of Burma Science and Technology Journal 3, 75–90.

Maung Maung, Thaung Htike, Tsubamoto, T., Suzuki, H., Chit Sein, Egi, N., Win, Z., Maung, T.Z.M., Ko, A.A., 2005. Stratigraphy of the primate-bearing beds of the Eocene Pondaung Formation at Paukkaung area, Myanmar. Anthropological Science 113, 11–15. https://doi.org/10.1537/ase.04S002

Maurin, T., Rangin, C., 2009. Structure and kinematics of the Indo-Burmese Wedge: Recent and fast growth of the outer wedge: Growth of the Outer Burmese Wedge. Tectonics 28, n/a-n/a. https://doi.org/10.1029/2008TC002276

Metcalfe, I., 1996. Pre-Cretaceous evolution of SE Asian terranes. Geological Society Special Publication 106, 97–122. https://doi.org/10.1144/GSL.SP.1996.106.01.09

Mitchell, A.H.G., 1981. Phanerozoic plate boundaries in mainland SE Asia, the Himalayas and Tibet. Journal of the Geological Society 138, 109–122. https://doi.org/10.1144/gsjgs.138.2.0109

Mitchell, A.H.G., 1989. The Shan Plateau and Western Burma: Mesozoic-Cenozoic Plate Boundaries and Correlations with Tibet 567–568.

Mitchell, A.H.G., 1993. Cretaceous-Cenozoic tectonic events in the western Myanmar (Burma)-Assam region. Journal of the Geological Society 150, 1089–1102. https://doi.org/10.1144/gsjgs.150.6.1089

Mitchell, A., Chung, S.-L., Oo, T., Lin, T.-H., Hung, C.-H., 2012. Zircon U–Pb ages in Myanmar: Magmatic–metamorphic events and the closure of a neo-Tethys ocean? Journal of Asian Earth Sciences 56, 1–23. https://doi.org/10.1016/j.jseaes.2012.04.019

Mitchell, A., Htay, M.T., Htun, K.M., 2015. The medial Myanmar suture zone and the Western Myanmar–Mogok foreland. Journal of the Myanmar Geosciences Society 6, 73–88.

Mitchell, A.H.G., 2017. Geological Belts, Plate Boundaries, and Mineral Deposits in Myanmar 105, 287 524-288. https://doi.org/10.2138/am-2020-B10521

Morley, C.K., Searle, M., 2017. Regional tectonics, structure and evolution of the Andaman-Nicobar Islands from ophiolite formation and obduction to collision and back-arc spreading. Geological Society Memoir 47, 51–74. https://doi.org/10.1144/M47.5

Morley, C.K., Tin Tin Naing, Searle, M., Robinson, S.A., 2020. Structural and tectonic development of the Indo-Burma ranges. Earth-Science Reviews 200, 102992. https://doi.org/10.1016/j.earscirev.2019.102992

Naing Htun Lin., Guo, Y., Wai, S.N., Tamehe, L.S., Wu, Z., Naing, N.M., Zhang, J., 2019. sandstones from the western Salin Sub-Basin, the Central Myanmar Basin: Implications for provenance, source area weathering, paleo-oxidation and paleo-tectonic setting. Journal of Asian Earth Sciences 22.

Najman, Y., Allen, R., Willett, E.A.F., Carter, A., Barfod, D., Garzanti, E., Wijbrans, J., Bickle, M.J., Vezzoli, G., Ando, S., Oliver, G., Uddin, M.J., 2012. The record of Himalayan erosion preserved in the sedimentary rocks of the Hatia Trough of the Bengal Basin and the Chittagong Hill Tracts, Bangladesh. Basin Res 24, 499–519. https://doi.org/10.1111/j.1365-2117.2011.00540.x

Najman, Y., Mark, C., Barfod, D.N., Carter, A., Parrish, R., Chew, D., Gemignani, L., 2019. Spatial and temporal trends in exhumation of the Eastern Himalaya and syntaxis as determined from a multitechnique detrital thermochronological study of the Bengal Fan. GSA Bulletin 131, 1607–1622. https://doi.org/10.1130/B35031.1

Najman, Y., Sobel, E.R., Millar, I., Stockli, D.F., Govin, G., Lisker, F., Garzanti, E., Limonta, M., Vezzoli, G., Copley, A., Zhang, P., Szymanski, E., Kahn, A., 2020. The exhumation of the Indo-Burman Ranges, Myanmar. Earth and Planetary Science Letters 530, 115948. https://doi.org/10.1016/j.epsl.2019.115948

Pearce, N.J.G., Perkins, W.T., Westgate, J.A., Gorton, M.P., Jackson, S.E., Neal, C.R., Chenery, S.P., 1997. A compilation of new and published major and trace element data for NIST SRM 610 and NIST SRM 612 glass reference materials. Geostandards Newsletter 21, 115–144. https://doi.org/10.1111/j.1751-908X.1997.tb00538.x

Pilgrim, G.E., 1916. Some newly discovered Eocenemammals from Burma. Records of the Geological Survey of India 47, 42–77.

Pivnik, D.A., Tuck, R.S., Nahm, J., 1998. Polyphase Deformation in a Fore-Arc/Back-Arc Basin, Salin Subbasin, Myanmar (Burma). AAPG bulletin 82 (1998). https://doi.org/10.1306/1D9BD15F-172D-11D7-8645000102C1865D

Racey, A., Ridd, M.F., 2015. Petroleum geology of Myanmar. Geological Society of London, 978-1-86239-735-4

Robinson, R.A.J., Brezina, C.A., Parrish, R.R., Horstwood, M.S.A., Nay Win Oo, Bird, M.I., Myint Thein, Walters, A.S., Oliver, G.J.H., Zaw, K., 2014. Large rivers and orogens: The evolution of the Yarlung Tsangpo-Irrawaddy system and the eastern Himalayan syntaxis. Gondwana Research 26, 112–121. https://doi.org/10.1016/j.gr.2013.07.002

Satyabala, S.P., 2003. Oblique plate convergence in the Indo-Burma (Myanmar) subduction region. Pure and Applied Geophysics 160, 1611–1650. https://doi.org/10.1007/s00024-003-2378-0

Saw Lwin, 1999. Petrological analysis of the rock samples collected by the Pondaung Fossils Expedition Team. Proceedings of the Pondaung Fossils Expedition Team.

Searle, M.P., Noble, S.R., Cottle, J.M., Waters, D.J., Mitchell, A.H.G., Hlaing, T., Horstwood, M.S.A., 2007. Tectonic evolution of the Mogok metamorphic belt, Burma (Myanmar) constrained by U-Th-Pb dating of metamorphic and magmatic rocks: U-Th-Pb Ages of Mogok Belt. Tectonics 26, n/a-n/a. https://doi.org/10.1029/2006TC002083

Searle, M.P., Morley, C.K., Waters, D.J., Gardiner, N.J., Htun, U.K., Than Than Nu, Robb, L.J., 2017. Chapter 12 Tectonic and metamorphic evolution of the Mogok Metamorphic and Jade Mines belts and ophiolitic terranes of Burma (Myanmar). Geological Society, London, Memoirs 48, 261–293. https://doi.org/10.1144/M48.12

Searle, M.P., Garber, J.M., Hacker, B.R., Htun, K., Gardiner, N.J., Waters, D.J., Robb, L.J., 2020. Timing of Syenite-Charnockite Magmatism and Ruby and Sapphire Metamorphism in the Mogok Valley Region, Myanmar. Tectonics 39. https://doi.org/10.1029/2019TC005998

Sevastjanova, I., Hall, R., Rittner, M., Paw, S.M.T.L., Naing, T.T., Alderton, D.H., Comfort, G., 2016. Myanmar and Asia united, Australia left behind long ago. Gondwana Research 32, 24–40. https://doi.org/10.1016/j.gr.2015.02.001

Shi, G., Cui, W.Y., Liu, J., Yu, H.X., 2001. Petrology of jadeite-bearing serpentinized peridotite and its country rocks from Northwestern Myanmar (Burma). Acta Petrologica Sinica 17, 483–490.

Shi, G., Cui, W., Cao, S., Jiang, N., Jian, P., Liu, D., Miao, L., Chu, B., 2008. Ion microprobe zircon U–Pb age and geochemistry of the Myanmar jadeitite. Journal of the Geological Society 165, 221–234. https://doi.org/10.1144/0016-76492006-119

Shi, G., Harlow, G.E., Wang, Jing, Wang, Jun, Enoch, N.G., Wang, X., Cao, S.M., Enyuancui, W., 2012. Mineralogy of jadeitite and related rocks from Myanmar: a review with new data. ejm 24, 345–370. https://doi.org/10.1127/0935-1221/2012/0024-2190

Singh, A.K., 2009. High-Al chromian spinel in peridotites of Manipur Ophiolite Complex, Indo-Myanmar Orogenic Belt: implication for petrogenesis and geotectonic setting. Current Science 96, 973–978.

Singh, A.K., 2013. Petrology and geochemistry of Abyssal Peridotites from the Manipur Ophiolite Complex, Indo-Myanmar Orogenic Belt, Northeast India: Implication for melt generation in mid-oceanic ridge environment. Journal of Asian Earth Sciences 66, 258–276. https://doi.org/10.1016/j.jseaes.2013.02.004

Sláma, J., Košler, J., Condon, D.J., Crowley, J.L., Gerdes, A., Hanchar, J.M., Horstwood, M.S.A., Morris, G.A., Nasdala, L., Norberg, N., Schaltegger, U., Schoene, B., Tubrett, M.N., Whitehouse, M.J., 2008. Plešovice zircon - A new natural reference material for U-Pb and Hf isotopic microanalysis. Chemical Geology 249, 1–35. https://doi.org/10.1016/j.chemgeo.2007.11.005

Soibam, I., Khuman, M.C., Subhamenon, S.S., 2015. Ophiolitic rocks of the Indo-Myanmar Ranges, NE India: Relicts of an inverted and tectonically imbricated hyper-extended continental margin basin? Geological Society Special Publication 413, 301–331. https://doi.org/10.1144/SP413.12

Steckler, M.S., Akhter, S.H., Seeber, L., 2008. Collision of the Ganges–Brahmaputra Delta with the Burma Arc: Implications for earthquake hazard. Earth and Planetary Science Letters 273, 367–378. https://doi.org/10.1016/j.epsl.2008.07.009

Strnad, L., Mihaljevič, M., 2005. Sedimentary provenance of Mid-Devonian clastic sediments in the Teplá-Barrandian Unit (Bohemian Massif): U-Pb and Pb-Pb geochronology of detrital zircons by laser ablation ICP-MS. Mineralogy and Petrology 84, 47–68. https://doi.org/10.1007/s00710-004-0057-1

Stuart, M., 1912. The geology of the Henzada district, Burma. Records of the Geological Society of India 41, 240–253.

Suzuki, H., Maung, M., Naing Soe, A., Shigehara, N., 2006. Lithostratigraphy of the Pondaung Formation (Eocene) between Tabyin and Kyauktakha to the west of Pauk, central Myanmar. Asian Primatology 4, 75–97. https://doi.org/10.1017/CBO9781107415324.004

Takai, M., Shigehara, N., Aung, A.K., Tun, S.T., Soe, A.N., Tsubamoto, T., Thein, T., 2001. A new anthropoid from the latest middle Eocene of Pondaung, central Myanmar. Journal of Human Evolution 40, 393–409. https://doi.org/10.1006/jhev.2001.0463

Tankard, A.J., Balkwill, H.R., Mehra, A., Din, A., 1994. Tertiary Wrench Tectonics and Sedimentation in the Central Basin of Myanmar.

Than Htut, 2017. Chapter 11 Myanmar petroleum systems, including the offshore area. Geological Society, London, Memoirs 48, 219–260. https://doi.org/10.1144/M48.11

Than Nyunt, Chit Saing, 1978. Onshore the sedimentary Basins of Burma: Central Basin, Arakan-Chin-Naga Yoma Basin. ESCAFE, Stratigraphic Correlation Program, Bur 2, 6–10.

Thet Tin Nyunt, Hans-Joachim Massonne, Tay Thye Sun, 2017. Chapter 13 Jadeitite and other high-pressure metamorphic rocks from the Jade Mines Belt, Tawmaw area, Kachin State, northern Myanmar. Geological Society, London, Memoirs 48, 295–315. https://doi.org/10.1144/M48.13

Tsubamoto, T., Takai, M., Shigehara, N., Egi, N., Tun, S.T., Aung, A.K., Maung, M., Danhara, T., Suzuki, H., 2002. Fission-track zircon age of the Eocene Pondaung Formation, Myanmar. Journal of Human Evolution 42, 361–369. https://doi.org/10.1006/jhev.2001.0543

Vredenburg, E., 1921. Results of a Revision of Some Portions of Dr. Noetling's Second Monograph of the Tertiary Fauna of Burma, Records of the Geological Survey of India. Geological Survey of India.

Wandrey, C.J., 2006. Eocene to Miocene Composite Total Petroleum System, Irrawaddy-Andaman and North Burma Geologic Provinces, Myanmar, Chapter E in Wandrey CJ,(ed.), Petroleum systems and related geologic studies in Region 8. South Asia: US Geological Survey Bulletin2208-E.

Wang, J.-G., Wu, F.-Y., Tan, X.-C., Liu, C.-Z., 2014. Magmatic evolution of the Western Myanmar Arc documented by U–Pb and Hf isotopes in detrital zircon. Tectonophysics 612–613, 97–105. https://doi.org/10.1016/j.tecto.2013.11.039

Westerweel, J., Roperch, P., Licht, A., Dupont-Nivet, G., Win, Z., Poblete, F., Ruffet, G., Swe, H.H., Thi, M.K., Aung, D.W., 2019. Burma Terrane part of the Trans-Tethyan arc during collision with India according to palaeomagnetic data. Nat. Geosci. 12, 863–868. https://doi.org/10.1038/s41561-019-0443-2

Westerweel, J., Licht, A., Cogné, N., Roperch, P., Dupont-Nivet, G., Kay Thi, M., Swe, H.H., Huang, H., Win, Z., Wa Aung, D., 2020. Burma Terrane Collision and Northward Indentation in the Eastern Himalayas Recorded in the Eocene-Miocene Chindwin Basin (Myanmar). Tectonics 39. https://doi.org/10.1029/2020TC006413

Win Swe, 1981. A major strike-slip fault in Burma. Contributions to Burmese Geology 1, 63–72.

Xie, J.-C., Zhu, D.-C., Dong, G., Zhao, Z.-D., Wang, Q., Mo, X., 2016. Linking the Tengchong Terrane in SW Yunnan with the Lhasa Terrane in southern Tibet through magmatic correlation. Gondwana Research 39, 217–229. https://doi.org/10.1016/j.gr.2016.02.007

Yao, W., Ding, L., Cai, F., Wang, H., Xu, Q., Zaw, T., 2017. Origin and tectonic evolution of upper Triassic Turbidites in the Indo-Burman ranges, West Myanmar. Tectonophysics 721, 90–105. https://doi.org/10.1016/j.tecto.2017.09.016

Zhang, J., Xiao, W., Windley, B.F., Wakabayashi, J., Cai, F., Sein, K., Wu, H., Naing, S., 2018. Multiple alternating forearc- and backarc-ward migration of magmatism in the Indo-Myanmar Orogenic Belt since the Jurassic: Documentation of the orogenic architecture of eastern Neotethys in SE Asia. Earth-Science Reviews 185, 704–731. https://doi.org/10.1016/j.earscirev.2018.07.009

Zhang, P., Mei, L., Hu, X., Li, R., Wu, L., Zhou, Z., Qiu, H., 2017. Structures, uplift, and magmatism of the Western Myanmar Arc: Constraints to mid-Cretaceous-Paleogene tectonic evolution of the western Myanmar continental margin. Gondwana Research 52, 18–38. https://doi.org/10.1016/j.gr.2017.09.002

Zhang, P., Najman, Y., Mei, L., Millar, I., Sobel, E.R., Carter, A., Barfod, D., Dhuime, B., Garzanti, E., Govin, G., Vezzoli, G., Hu, X., 2019. Palaeodrainage evolution of the large rivers of East Asia, and Himalayan-Tibet tectonics. Earth-Science Reviews 192, 601–630. https://doi.org/10.1016/j.earscirev.2019.02.003

Credit Author Statement

Joseph McNeil: Conceptualization, Software, Validation, Investigation, Data Curation, Writing – Original Draft, Writing - Review & Editing, Visualisation; **Amy Gough**: Conceptualization, Validation, Resources, Writing - Review & Editing, Supervision, Funding Acquisition, Project Administration; **Robert Hall**: Conceptualization, Writing - Review & Editing, Supervision, Funding Acquisition, Project Administration; **Nils K. Lünsdorf**: Software, Data Curation, Resources, Writing - Review & Editing, Supervision; **Max Webb**: Data Curation, Resources; **Sarah Feil**: Data Curation

Declaration of interests

☒ The authors declare that they have no known competing financial interests or personal relationships that could have appeared to influence the work reported in this paper.

☐The authors declare the following financial interests/personal relationships which may be considered as potential competing interests:

Figure 1: A schematic geological map of Myanmar, showing the primary terranes and their spatial relations to each other (modified from Westerweel, 2019 and Licht et al., 2015). The Myanmar border is shown by the white dotted line. The location of figure 2 is shown by the red box. IMR: Indo-Myanmar Ranges, MMB: Mogok Metamorphic Belt, SMR: Sino-

Myanmar Ranges, SSB: Salin Sub-basin, PSB: Pyay Sub-basin, CB: Chindwin Sub-basin, PYSB: Pegu-Yoma Sub-basin, SMSB: Shwebo Sub-basin, ETP: Eastern Tibetan Plateau, GB: Gangdese Batholith, SF: Sagaing Fault, KF: Kabaw Fault, WB: Western Ophiolite Belt, EB: Eastern Ophiolite Belt, JM: Jade Mines Belt, SSI: Shan Scarp Intrusions, DB: Dianxi Batholith.

Figure 2: Simplified geological map of the Salin Sub-basin (modified from Licht et al., 2015 and Pivnik et al., 1998), showing the locations of Cenozoic sedimentary deposits relative to the Indo-Myanmar Ranges and Sino-Myanmar Ranges (SMR), and the major faults (red, displacement indicated by arrows and ticks), as well as the sample locations and numbers. Sample locations marked with a red dot are from the 2017 field season (samples starting MAG_17), and samples marked with a light blue dot are from the 2018 field season (samples starting MAG_18).

Figure 3: Summary of the chronostratigraphy, lithostratigraphy, and thicknesses of the formations in this study, as well as the stratigraphic location of the samples.

Figure 4: Field images depicting typical outcrops of a) the Shwezetaw Formation, here displaying parallel-bedded medium-fine sandstones, and b) the Padaung Formation, displaying finely-interbedded sands and silts.

Figure 5: a) QFL plot after (Dickinson et al., 1983) showing the quartz, feldspar and lithic fragment proportions within each sample. All samples, except the ‘dissected arc’ Middle Padaung sample, plot within the Recycled Orogen field. b) QmFLt plot after (Folk, 1980) showing the monolithic quartz, feldspar and lithic fragment proportions within each sample. All samples are feldspathic litharenite, with the exception of the Shwezetaw-Padaung Formation sample, which is a litharenite.

Figure 6: Heavy mineral assemblages shown as bar graphs, shown in stratigraphic order. The number of ‘good hit’ grains included in each sample are displayed to the right of the bars.

Figure 7: Histogram plots of detrital zircon ages collected in this study. Multiple samples from the same formations have been grouped together to identify overall trends.

Figure 8: Cathodoluminescence images of zircon grains representative of their samples, showing their morphologies, ages and internal structures. A) 6 grains from the Pondaung Formation (MAG_17_03), B) 9 grains from the Shwezetaw Formation (MAG_17_04), C) 14 grains from the Shwezetaw-Padaung Formation boundary (MAG_17_19), D) 12 grains from the Padaung Formation (MAG_17_21). Zircons with labels were analysed; discordant grains are marked with an asterisk (*). The scale is the same for all frames.

Figure 9: Comparative histograms showing combined U-Pb ages from terranes and regions around the Central Myanmar Basin. A) Padaung Formation (this study), B) Shwezetaw Formation (this study), C) Pondaung Formation (this study), D) Mogok Metamorphic Belt Intrusions, E) Wuntho-Popa Arc, F) Sodon Pluton, G) Western Ophiolite Belt (IMR), H) Chin Hills (IMR), I) Pane Chuang Formation (IMR), J) Map showing the approximate sampling locations of the histograms. Age compilations and sources are available in Supplementary Table 3.

Figure 10: Block diagrams depicting the Salin Sub-basin at three different time periods, highlighting the depositional environment and relative sedimentary contributions from the surrounding terranes. A) Pondaung Formation: Priabonian woodland and floodplain areas with westward-directed deltaics. The primary sources are a metamorphic source in the basement rocks of northern Myanmar including the Jade Mines Belt (JMB) and Eastern Ophiolite Belt (EOB), as well as a strong signal from the recently volcanics of the Wuntho-Popa Arc (WPA). The Indo-Myanmar Ranges (IMR) are not a significant topographic feature at this time, so do not contribute any sediment. B) Shwezetaw Formation: a Rupelian tidal-dominated fluvio-marine environment with a stable provenance regime. Sediment is sourced in the Chin Hills (CH) and Pane Chuang Formation (PCF) in the IMR, and as before in northern Myanmar. The Mogok Metamorphic Belt (MMB) may be sources at this time and/or the older WPA volcanics could also be providing sediment. C) Padaung Formation: a Rupelian fluvial-tidal deltaic system in the north, that passes southwards into a shallow marine environment in the medial and southern sections of the basin. Provenance is less stable than in the Shwezetaw Formation, with multiple tributaries variously providing sediment from the IMR, northern Myanmar, and the Late Cretaceous sections of the WPA. Input from the MMB or 50-70 Ma sections of the WPA is reduced, suggesting the presence of a topographic barrier (such as the uplift of the WPA proposed in Zhang et al., 2017), or progressive burial of the WPA respectively. Depositional environment reconstructions in Gough et al., 2020.

Figure 11: Early Oligocene plate reconstruction showing the configuration of major crustal blocks at around 33 Ma, modified from the 40 Ma (Eocene) reconstruction in Westerweel et al. (2020). The location of the Salin Sub-basin (SSB) is shown by the red star. Our proposed schematic sediment pathway is shown in blue and approximately represents the river system that existed during deposition of the Shwezetaw Formation. River headwaters are in northern Myanmar, with further catchments in the Jade Mines Belt, Eastern Ophiolite Belt, Indo-Myanmar Ranges Wuntho-Popa Arc, and possibly, the Mogok Metamorphic Belt. The Indo-Myanmar Ranges have become a significant topographic feature at this point and provide substantial amounts of material to the SSB. The main river is shown to flow primarily south along the length of the backarc basin, but alternatively, it may also have flowed along sections of the forearc basin. The SSB is shown as being topographically divided from the Chindwin Basin (CB) to the north, which records an unconformity during the time of deposition of the Shwezetaw and Padaung Formations in the SSB.

- U-Pb detrital zircon and heavy mineral data suggest numerous local sources.
- Main sources include the Indo-Myanmar Ranges, Wuntho-Popa Arc and Myanmar basement.
- Presently buried arc material and/or the Mogok Metamorphics are possible sources.
- Increasing proportions of Cr-spinel could record uplift of the Indo-Myanmar Ranges.
- The Indo-Myanmar Ranges were a prominent source of sediment by the mid-Oligocene.